Adaptively monitoring streamflow using a stereo computer vision system

Nicholas Reece Hutley[1], Ryan Beecroft[1], Daniel Wagenaar[2], Josh Soutar[3], Blake Edwards[4], Nathaniel Deering[1], Alistair Grinham[1], and Simon Albert[1]

[1]School of Civil Engineering, The University of Queensland, Brisbane 4072, Australia
[2]Xylem Water Solutions, Newcastle 2292, Australia
[3]Xylem Water Solutions, Brisbane 4174, Australia
[4]Leading Edge Engineering Solutions, Albury 2640, Australia

Correspondence: Nicholas Reece Hutley (nicholas.hutley@uq.net.au)

Abstract. The gauging of free surface flows in waterways provides the foundation for monitoring and managing the water resources of built and natural environments. A significant body of literature exists around the techniques and benefits of optical surface velocimetry methods to estimate flows in waterways without intrusive instruments or structures. However, to date, the operational application of these surface velocimetry methods has been limited by site configuration and inherent challenging optical variability across different natural and constructed waterway environments. This work demonstrates a significant advancement in the operationalisation of non-contact stream discharge gauging applied in the computer vision stream gauging (CVSG) system through the use of methods for remotely estimating water levels and adaptively learning discharge ratings over time. A cost-effective stereo camera-based stream gauging device (CVSG device) has been developed for streamlined site deployments and automated data collection. Evaluations between reference state-of-the-art discharge measurement technologies using DischargeLab (using surface structure image velocimetry), Hydro-STIV (using space–time image velocimetry), acoustic Doppler current profilers (ADCPs), and gauging station discharge ratings demonstrated that the optical surface velocimetry methods were capable of estimating discharge within a 5 %–15 % range between these best available measurement approaches. Furthermore, results indicated model machine learning approaches leveraging data to improve performance over a period of months at the study sites produced a marked 5 %–10 % improvement in discharge estimates, despite underlying noise in stereophotogrammetry water level or optical flow measurements. The operationalisation of optical surface velocimetry technology, such as CVSG, offers substantial advantages towards not only improving the overall density and availability of data used in stream gauging, but also providing a safe and non-contact approach for effectively measuring high-flow rates while providing an adaptive solution for gauging streams with non-stationary characteristics.

1 Introduction

Globally, hydrological flow occurs through natural and man-made open channels and floodplains, often transporting life-sustaining water to ecosystems and civilisations (Herrera et al., 2017; Albert et al., 2017, 2021; Grinham, 2007; Prüss-Ustün et al., 2014). Likewise, rainfall variability with increasing risk due to climate change can cause extreme flows (Lehmann et al., 2015; Palmer and Räisänen, 2002) resulting in significant economic, environmental, and life losses (Gaume et al., 2009; Grinham et al., 2012), as well as an increasing risk of extreme drought events into the future (Park et al., 2021; Li et al., 2016). Within this context the field of hydrography endeavours to monitor and understand the dynamics of flows in these waterways through space and time (Westerberg et al., 2016; Kuentz et al., 2017; Mcmillan et al., 2012). From designing infrastructure intersecting with waterways (Lindow and Curtis, 2010), to budgeting water security

(Daly et al., 2019; Sene et al., 2018) and improving forecasting models for near and long-term policy planning (Hering et al., 2015; Hutley et al., 2020), gauging waterways continues to be an important utility for society with substantial time, human risk, investment, and maintenance funding worldwide (Crochemore et al., 2020).

There are many operational and emerging methods for waterway gauging, varying widely in cost, accuracy, reliability, and risk (Tauro et al., 2016, 2018; Gordon, 1989; Costa et al., 2000; Yang et al., 2020). Intrusive methods range from the resource-intensive installation of hydraulic control structures to measure discharge rates analytically using simpler water level measurements within a designed range by obstructing and controlling the flow through a standardised geometry (Boiten, 2002) (often to the detriment of aquatic species (Mueller et al., 2011), as well as sedimentation and erosion (Pagliara and Palermo, 2015; Ogden et al., 2011), through to the risking of people and equipment entering the stream to measure velocities using passive mechanical current meters or active acoustic Doppler velocimetry profiles (Gordon, 1989).

In order to estimate discharges through a waterway without the flow passing through the geometry of a known hydraulic control structure, other methods largely rely on the measurement of velocities across the channel and integrating these estimated velocities through the cross-sectional area using some binned resolution (Herschy, 1993). Measuring these velocities within the cross section CE1 of waterways is fraught with various challenges, including limitations in measuring close to boundaries, debris, vegetation, aeration, unsteady flows, equipment damage, and safety risks (Petrie et al., 2013; Lee et al., 2014; Klema et al., 2020; Harding et al., 2016). Furthermore, the ongoing measurements of velocities in a waterway are difficult and expensive to carry out and maintain, especially during flood events (Banasiak and Krzyżanowski, 2015). Therefore, the development of discharge ratings (relating water level to an estimated discharge) have become commonplace through the construction of (often still expensive to build and maintain) gauging structures and stilling wells. This approach allows the more easily measured water level over time to be converted to discharge estimates through a fitting of manual discharge measurements recorded routinely and/or opportunistically over decades by professional hydrographers.

In practice, the common approach to gauging streams using fitted discharge ratings presents challenges for obtaining unbiased measurements of non-stationary channel environments over time, particularly when significant flow events cause changes to natural waterways (Birgand et al., 2013; Tomkins, 2014; Guerrero et al., 2012; Jalbert et al., 2011; Di Baldassarre and Montanari, 2009). Therefore, non-contact and affordable solutions such as radar (Rahman Khan et al., 2021) or optical offer the potential to overcome these challenges by measuring velocity and stage without in situ sensors. Similar to one of the oldest manual methods to measure

velocities in a waterway by measuring the displacements of surface floats over time, the passive optical measurement of surface velocities using relatively inexpensive camera systems has been an attractive approach to stream gauging (Dobriyal et al., 2017). Despite the documented advantages of this approach (Dramais et al., 2011) coupled with its potential for affordable scalability to decrease monitoring sparsity, traditional gauging approaches have not yet been replaced or augmented by a widespread adoption of optical surface velocimetry after 20 years of active research (Tauro et al., 2018). Optical surface velocimetry in the form of large-scale particle image velocimetry (LSPIV) and space–time image velocimetry (STIV) are well-established approaches for estimating streamflow (Fujita and Komura, 1994; Watanabe et al., 2021). Whilst operationalised systems using LSPIV exist (Bechle et al., 2012) using cross-correlation of sequential image vector fields, surface structure image velocimetry (SSIV) is a derivative of LSPIV that filters the background, enhancing the moving surface structures (Leitão et al., 2018). SSIV has been applied in the DischargeLab analysis software and DischargeKeeper operational monitoring system reaching technology readiness level (TRL) 9 in use internationally with the ability to apply optical water level detection techniques with varying success without the use of a vertical gauging reference structure in the water (Photrack AG, Zürich, Switzerland) (Peña-Haro et al., 2021). Similarly, STIV quantifies the change in luminance variation through time across one-dimensional search lines defined in parallel to the stream flow (Fujita et al., 2007). Whilst the majority of STIV trials have been part of research efforts, the approach has been packaged into user-friendly Hydro-STIV software (Hydro Technology Institute Co., Ltd.) and is being deployed by numerous organisations globally, particularly using unmanned aerial vehicles (UAVs) (Koutalakis et al., 2019). The central challenges with the application of these approaches remain the reliance on an externally measured water level, accurate ground control reference points assigned to fixed pixels in the frame for accurate vector transformation, and a moderate degree of expertise required to manually tune site-specific settings to reduce errors from changes in the site environment and lighting conditions in the initial setup CE2 (Detert, 2021).

The existing barriers to widespread implementation of optical stream gauging include initial surveying and calibration of new sites, development of system integration, and difficulties in measuring velocities reliably with surface tracers across different site flow conditions, water clarity, and lighting environments (Pizarro et al., 2020). This study aims to develop and evaluate a significant advance towards a rapidly deployable, accessible, automated operational, and scalable optical stream gauging system with improved reliability for gauging streams across varying flow and lighting conditions. With increasing successful developments in a range of methods in optical surface velocimetry, recent technological advancements in optical technologies for capturing

videos, surveying environments, and computer vision analysis, along with technical advancements in embedded computing power efficiency, communications, and cloud computing and storage services, we anticipate optical approaches to
stream gauging will further transition from the research domain towards the operational domain.

2   Methods

To address the study aim, the methodology firstly presents the operation of the computer vision stream gauging (CVSG) system and the process for site setup and configuration. Stereographic remote water level estimation approaches and adaptive cross-sectional learning with rectification to coordinates of the water surface are then outlined. The optical flow technique used by CVSG for estimating surface velocities is then described along with the approach for learning the surface velocity distributions over multiple measurements under different optical conditions and fitting these surface velocity measurements to a model of the surface velocity profile transformed into a function of a boundary distance factor. Thereafter, the principles for the development of adaptive learning discharge ratings are detailed, followed by a summary of the reference operational discharge estimation approaches applied in this study. Finally, the characteristics of the optical flow field study sites and the stream gauging field sites demonstrated in this work are presented.

2.1   Computer vision stream gauging system

The CVSG system employed in this study was developed for use in capturing stereo videos of waterways with automated processing of these into estimates of the water level, surface velocities, and gauged discharges. Figure 1 outlines the operational process of the CVSG system. The CVSG hardware has been designed around the use of a ZED 2/2i stereo camera (Stereolabs Inc., San Francisco, CA, USA) with or without internal infrared filters and a NVIDIA Jetson Xavier NX (NVIDIA Co., Santa Clara, CA, USA). The total power consumption of the CVSG hardware collecting data in this study was on the order of $36\,\mathrm{W\,h\,d^{-1}}$, averaging $1.5\,\mathrm{W}$ with a peak power draw of $30\,\mathrm{W}$. A sliding lens mechanism is inbuilt to allow for switching between different light wavelength band filters to enhance night measurements and collect data for discerning variables of water quality, such as suspended sediments. The system also employs a cloud architecture for automated data handling and internet of things (IoT) fleet management in managing the configuration of CVSG devices and sites drawing from a range of internal and external data sources. The integration of modern cloud analytics and fleet management allows for artificially intelligent predictive and adaptive sampling. Under typically configured baseflow conditions, the device operates at a sampling frequency of 60 min, capturing a video duration ranging between 3 and 30 s. During rapid rises in streamflow, the system can rapidly adapt and increase sampling frequency to between 2 and 15 min (depending on bandwidth and power conditions) to increase data density in less certain regions of the discharge rating.

Placing a CVSG device perpendicular or parallel with a waterway and configuring the upstream and downstream boundary distances relative to the camera that defines the region to be analysed is sufficient for the system to begin estimating the level of any water within 40 m in view of the camera. Then, using the inertial measurement unit (IMU), the accelerometer provides the orientation of the camera relative to gravity and then projects the estimated planar water surface into the image space for rectified surface velocities in this plane to be estimated at 0.1 m resolution across the cross section using an optical flow algorithm. The optical resolution of the flow in metres per pixel is calculated based on the water surface projection in order to filter any motions in the area of the field of view beyond the limits of acceptable optical flow resolution accuracy (normally limited to a maximum of 0.05 m per pixel up to 0.2 m per pixel). Beyond this, providing the bathymetry of the cross section and the camera's two-dimensional location (horizontal and vertical coordinates) relative to the reference frame of the cross-sectional data allows the system to begin learning a cross-sectional model of the ground at a site, as well as fitting the model of surface velocity profiles, estimating discharge, and adaptively learning a discharge rating through hundreds and thousands of recordings at a site over time. Site configurations are stored and referenced in time series, allowing for site configuration changes through time, typically from updated manual cross-sectional surveys or changes to the camera location. It is possible to set up the system with a cross section without knowledge of a surveyed location of the camera. Cross-sectional data can be referenced to the camera location visually through the projection of the cross-sectional data into the image overlay and tuning the predicted location of the camera to match the projection.

When videos are captured by the system, the analysis of these videos occurs in configured branches, allowing the simultaneous automated analysis of the same video using different configurations or water level data sources (e.g. the original stereo-derived water level estimation and an external water level sensor). Site coordinate systems are standardised with the x axis locally parallel to the waterway (positive in downstream direction), the y axis locally perpendicular to the waterway (positive away from or to the right of the camera), and the z axis aligned locally with the gravitational force measured by the camera. Cross-sectional data are one-dimensional and referenced to the y axis across the waterway. The analysis region is not needed to be directly in front of the camera but should be ideally a section of uniform and straight cross section in view (can be as small as 0.5 m along the stream and up to as large as visible and practicable for optical flow measurement). When selecting a site, care should
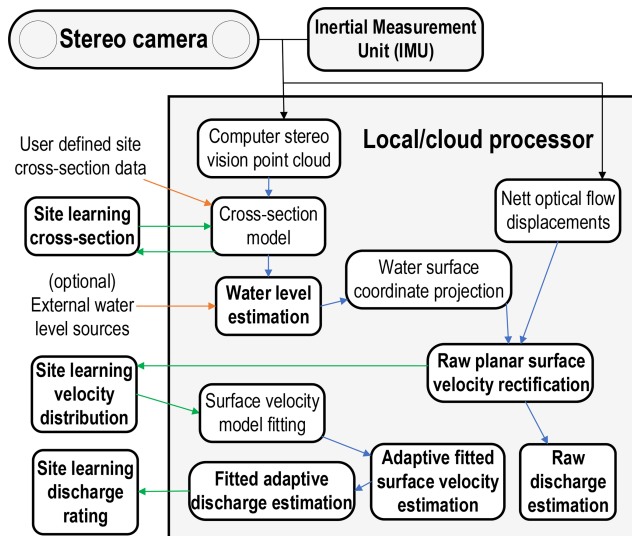
Figure 1. Computer vision stream gauging (CVSG) system operation diagram.

be taken to identify sites with suitable surface flow visibility and oriented south-facing (Southern Hemisphere) or north-facing (Northern Hemisphere) where possible to avoid sun glare, while keeping the horizon or sky outside of the cam-
[5] era field of view (maximising the water surface in the field of view and reducing automatic exposure determination from the sky). The CVSG system has been developed to balance ease of setup, ease of operation, affordability, accuracy of results, and reliability for stream gauging.

[10] ## 2.2 Stereo cross section and water level estimation

The primary driver for the use of a stereo camera in the CVSG device is the potential to use stereophotogrammetry to reduce the surveying requirements typically associated with surface velocimetry techniques for the rectification of pixel
[15] displacements into realistic spatial scales over a wide range of water levels. However, a stereo computer vision system also makes it possible to initially survey and then continuously monitor the terrain of the cross section above the water level for changes due to erosion, deposition, or vegetation
[20] and offers the potential advantage for measuring surface velocities on variable or steep hydraulic gradients. The adaptive learning of stream bank profiles over time allows for an advancement forward with non-stationary stream gauging in morphologically unstable sites. While the CVSG sys-
[25] tem maintains an adaptive cross-sectional database for each site which is compared and adapted with each measurement for visible terrain above the estimated water level (applying more weight to gradual changes in time and requiring many consistent measurements to gradually apply any ob-
[30] served dramatic changes in the cross-sectional profile), the results of this study applied fixed manual cross-sectional sur-

veys from the time of deployment over the entirety of the time periods evaluated.

Stereophotogrammetry is applied to estimate the distance from the camera to features which are matched between the [35] stereo pairs of rectilinear-corrected images where a convolutional neural network model (provided by the camera manufacturer, Stereolabs), that has been trained on pairs of stereo images, is applied to improve both the accuracy and solution density particularly with reflective and featureless sur- [40] faces. With a point cloud calculated for each video frame, the median coordinate is taken of each of the three coordinate dimensions of the point cloud for each recording analysed. Water level is estimated by scanning across the point cloud in 0.5 m wide lines within the configured stream cross- [45] sectional analysis region from the near bank towards the far bank. The median elevation between these cross-sectional scanning lines is taken, and the resulting cross-sectional profile is lastly filtered by a 0.5 m footprint median filter. After this, an iterative process constrains the near and far water [50] boundaries to ideally within the first 2 m (and not more than 10 m due to the effects of various optical conditions on the accuracy of the point cloud over the water surface) from the near bank across the water surface by moving the far boundary closer using similar pixels assumed to be water from the [55] RGB image frame while avoiding any obstructed view of the near bank. The first percentile of the elevation points of the stereophotogrammetry cross-sectional profile within this domain is then estimated as the water level (effectively taking the near minimum of the surface while reducing the impact [60] of any sporadic point cloud artefacts).

The CVSG system has also been developed with external water level data source aggregation and parallel analysis capability alongside stereo water level estimates. With an estimated water plane level relative to the camera position, [65] and an IMU (median filtered and stability tested for each recording) providing the orientation of the camera relative to gravity, as well as the camera's optical properties, the across stream coordinates of the water surface plane every 0.1 m are first projected and interpolated into the image pixel space. [70] Following this, the streamwise coordinates along the stream are predicted for each pixel spanning from the image (from the left lens in the camera's perspective) centreline.

2.3 Optical flow surface velocimetry estimation

The motions in the recorded videos are computed using the [75] Farneback algorithm (Farnebäck, 2002, 2003) to solve the energy-like minimisation problem for the optical flow equation across the pixel space between each pair of consecutively recorded frames. Whilst optical flow has previously been applied to the measurement of stream discharge (Perks, [80] 2020a; Khalid et al., 2019), there are different existing algorithms developed for reaching an optimal solution of the optical flow equation (Baker et al., 2011). Shi et al. (2020) compared three established and widely applied optical flow

techniques to breaking surges, noting the advantages of the Farneback algorithm for its relatively high accuracy and dense flow fields, as well as a lower sensitivity to noise with the converging iterative solution for the displacement vector, $\boldsymbol{d}$ TS1, between a pair of images using quadratic polynomials following Eq. (1):

$$
\begin{aligned}
\boldsymbol{d}(\boldsymbol{x}_{\text{im}}) = & \left(\sum_{\Delta \boldsymbol{x}_{\text{im}} \in \mathbf{I}_{\text{local}}} w \mathbf{A}^T \mathbf{A} \right)^{-1} \\
& \sum_{\Delta \boldsymbol{x}_{\text{im}} \in \mathbf{I}_{\text{local}}} w \mathbf{A}^T \Delta \boldsymbol{b}_f,
\end{aligned}
\tag{1}
$$

where $\mathbf{I}$ is the greyscale image with local neighbourhood regions denoted by $\mathbf{I}_{\text{local}}$ using the image coordinates $\boldsymbol{x}_{\text{im}}$ and y_{im} to form $\boldsymbol{x}_{\text{im}} = \begin{bmatrix} \boldsymbol{x}_{\text{im}} \\ y_{\text{im}} \end{bmatrix}$, where the change in brightness between the corresponding pixels in the pairs of images are denoted $\Delta \boldsymbol{x}_{\text{im}}$. Furthermore, w is a weighting function over the local neighbourhood regions, while the polynomials are defined by $f(\boldsymbol{x}_{\text{im}}, y_{\text{im}}) \cong a_1 + a_2 \boldsymbol{x}_{\text{im}} + a_3 y_{\text{im}} + a_4 \boldsymbol{x}_{\text{im}}^2 + a_5 y_{\text{im}}^2 + a_6 \boldsymbol{x}_{\text{im}} y_{\text{im}}$ with $\mathbf{A} = \begin{bmatrix} a_4 & \frac{a_6}{2}\text{TS2} \\ \frac{a_6}{2}\text{TS3} & a_5 \end{bmatrix}$, $\boldsymbol{b}_f = \begin{bmatrix} a_2 \\ a_3 \end{bmatrix}$ and $c = a_1$.

The approach is a variational method combining the assumptions of local neighbourhood brightness intensity variation between frames with the minimisation of an energy function assuming a slowly varying displacement field for locally smooth velocity gradients (Shah and Xuezhi, 2021). A four-level pyramid of processing steps (Adelson et al., 1984) is applied to estimate larger overall motions first at a coarser resolution, interpolating these larger motions to higher resolutions over the four steps refining the optical flow field with each step increasing in resolution up to the original video resolution (typically 1920×1080 recorded from each camera simultaneously).

With the optical flow algorithm applied to each pair of consecutively recorded frames, depending on the visual flow conditions there can be errors in the estimated motion between frames, camera vibrations, as well as natural or man-made motions occurring between the camera and the waterway surface to be measured. By summing the estimated optical flow fields over the duration of each recording and averaging the optical flow field stack produced to find the nett motions estimated over the duration of each recording, any oscillatory and non-continuous motions can be suppressed. While taking the median of the flow fields would be reasonably more preferable in this context, the average accumulating flow field computation is applied to reduce the edge computing hardware requirements of the method, particularly with memory usage, as the duration of the measurement scales the number of instantaneous flow field frames stored in memory for a median calculation. Taking the two-dimensional image space gradients of the previously computed streamwise (x) and cross-stream (y) coordinates of the water surface plane, the optical flow pixel displacement rates are scaled onto the water surface plane, noting that the optical flow motions in the horizontal and vertical directions of the image space can each be indirectly measuring components of both the streamwise and cross-stream motions on the water surface plane. From this point, the motions out of the assumed plane of the water surface are filtered out of the analysis to further remove false motions unrelated to the waterway surface velocities (such as animals and swinging ropes, which are not moving in the assumed plane of the water surface).

Assuming the remaining velocities over the length of the analysis section are velocities related to the motion of the water surface, and assuming a continuity in the uniformity of the analysis section length without transitional flows, the strongest detected velocities are collapsed into a single-dimensional raw cross-sectional surface velocity profile. The assumed continuity over the analysis section length facilitates the measurement of velocities across spatially inconsistent optical flow measurement and lighting conditions along the length of the analysed section.

Whilst the visual conditions for optical flow measurement can still be insufficient for reliable measurements across the length of the measurement section in all situations, the CVSG system then applies an adaptive learning velocity distribution across the cross section at 0.1 m intervals and references these learning measurements over the observed water level range at 0.01 m intervals. This process of developing an adaptive database of surface velocity measurements across the stream at different water levels (adaptive learning surface velocity distributions) allows the system to use multiple measurements of the same water level over time in different conditions to combine these measurements into a complete surface velocity profile while simultaneously being adaptive to observed changes in surface velocity profiles in non-stationary environments. Furthermore, there can still be biases present in these measurements over time which could take the form of incorrect velocity signals and sections of the cross section which are persistently in poor optical flow measurement conditions or entirely out of the range of the camera's pixel resolution in order to measure the displacements with any accuracy. In this case data gaps are filled by fitting the sufficiently measurable surface velocities to an exponential relationship model in a transformed spatial domain that scales with each measured surface velocity's relative distance to the boundaries of the flow according to Eq. (2):

$$
v_{\text{s}} = v_{\infty} \left(1 - e^{-bx} \right),
\tag{2}
$$

where v_{s} is the surface velocity, v_{∞} constrains the asymptote approaching the free stream velocity, b is a cross-sectional variable, and x is the boundary distance factor (defined here as the depth multiplied by the distance to the nearest water surface edge). The relationship in Eq. (2) bounds the surface velocity to zero either where the depth reaches zero or at the

intersection of the water surface and the cross section. By using the measured adaptive learning surface velocities distribution as data for automated fitting of the gap-filled surface velocity profile model across the entirety of the cross section, an estimated surface velocity profile consistent with the measurements collected at each water level is produced. The Trust Region Reflective algorithm (Branch et al., 1999) is used to optimise the least squares fit of these data by predicting the free stream velocity and cross-sectional variables fitting the measurements learned in the adaptive surface velocity distribution. Whilst the automated fitting of the surface velocity profile model assumes that the relationship between the measured surface velocities and the flow boundary are consistent across the cross section, this assumption is likely to weaken with significant variations in channel roughness across the cross section, particularly if the surface velocities neighbouring these regions of different roughness are not represented by samples in the adaptive surface velocity distribution.

2.4 Adaptive learning discharge rating

In order to estimate discharges from surface velocity profiles, an assumption is made in scaling the surface velocities to approximate the mean velocity profile across the cross section using a ratio, α, which is then integrated over the cross-sectional area at 0.1 m increments to estimate discharge. Hauet et al. (2018) examined the vertical profiles of 3611 gaugings from 176 sites with different bed types (concrete, sandy, pebbly, boulders), finding the primary driver of the ratio, α, to be the depth of flow. Their study found a linear trend for hydraulic radiuses above 1 m ($\alpha = 0.8$) up to 5 m ($\alpha = 0.9$), and furthermore it was concluded to use $\alpha = 0.8$ for depths less than 2 m and $\alpha = 0.9$ for depths greater than 2 m in natural channels. Following from this, the CVSG analysis applies a varying α across the cross section switching between a low (default 0.8) and high (default 0.9) value dependent on a threshold depth (default 2 m) at each 0.1 m interval. The result of this cross-section-varying depth-dependent approach is an effective α weighted on the distribution of depths within the cross section.

Using the adaptive learning surface velocity distributions and the associated fitted model surface velocity profiles, an adaptive discharge estimation is produced for each observed water level at 0.01 m intervals. This process is replicated independently in parallel for the lower and upper surface velocity and discharge estimates to produce an adaptive learning discharge rating envelope. The result of this is a new discharge rating envelope fitted to the latest discharge estimates across all of the observed water levels at a site with each new measurement. The learning discharge rating can be configured to either be generated from the range of discharge estimates by directly applying a locally fitted Savitzky–Golay signal filter (Savitzky and Golay, 1964) (using a filter window size of 0.05 m vertically with nearest boundaries and

linear fitting) or fitting a power law weighted by the number of observations and the optical flow coverage measured at each 0.01 m water level increment. The latter power law weighted fitting method has not been applied here, as the Savitzky–Golay signal filter is chosen instead for the results presented in this work (considered by the authors to be the preferred default configuration for general application, following the arguments of Fenton, 2018). Quality codes are automatically determined for each discharge estimate based on a function of the number of observations, the optical measurement coverage resulting from the lighting and seeding conditions, water level estimation, and convergence between the current measurement, the learning velocity distribution, the fitted surface velocity profile model, and the learning discharge rating.

2.5 Operational discharge estimation references

Results from the CVSG-derived discharge estimates in this study have been directly compared against the best available acoustic and optical methods for measuring discharge. As part of these reference technologies, two commercially available and well-developed technologies for estimating discharge using optical methods of measuring surface velocities have been applied. These analyses were undertaken by DischargeLab software (Photrack AG, Zürich, Switzerland) using surface structure image velocimetry (SSIV) (Leitão et al., 2018) and Hydro-STIV software (Hydro Technology Institute, Osaka, Japan) using space–time image velocimetry (STIV) (Fujita et al., 2007). Furthermore, the raw surface velocity results from these technologies have been processed using the surface velocity model fitting methodology used in the CVSG system that is presented here demonstrating the broader applicability of the methods presented in this study.

Acoustic Doppler current profilers (ADCPs) were utilised in order to estimate the subsurface velocities and produce reference acoustic estimates of the discharge independent of the optical approaches. Where available, ADCP velocity estimates closest to the surface (between 0.13 to 0.19 m depth) were compared to surface velocity estimates from the optical surface velocimetry technologies. Additionally, historical ADCP-derived estimates of discharge used to develop discharge ratings were utilised as a reference. The most up-to-date discharge rating fits published by government agencies based on the professional judgement of hydrographers using the applied technology and data available prior to the deployment of optical methods at each site were used to represent the best available estimates. These latest discharge rating fits at water level gauging station sites were then also used as a reference for time series comparisons through the conversion of the recorded water levels to the discharge predicted by the discharge rating fit. Although these different reference estimates have their own limitations and uncertainties, the comparison of the best available estimates at each case study site using the different technologies can provide

Figure 2. Images collected from study sites at **(a)** Castor River, Ontario, Canada (10 April 2019, 15:55 LT), **(b)** an irrigation channel, NSW, Australia (19 September 2020, 14:00 LT), **(c)** Tyenna River, Tasmania, Australia (5 March 2021, 12:12 LT), and **(d)** Paterson River, NSW, Australia (1 March 2022, 09:48 LT).

some insights both in where they differ and to what degree they agree. At two existing government-maintained gauging stations, historical manual gaugings have been compared along with CVSG, DischargeLab, and Hydro-STIV measurements relative to the latest published discharge rating using root mean square error (RMSE), the mean percentage difference, and the Nash–Sutcliffe efficiency (NSE) (Jackson et al., 2019) commonly applied for assessing predictive skill for discharges in hydrological settings due to its sensitivity to extreme values.

2.6   Field case study sites

This study includes four field case study sites (Fig. 2), inclusive of a single surface velocimetry benchmark time captured on the Castor River, Ontario, Canada (Perks et al., 2020b) and a single capture of an irrigation channel in New South Wales (NSW), Australia. Single points in time were focused on the optical method assessments relative to the available reference data for measuring surface velocities and estimating discharges. Two of the four sites presented here were continuously gauged with CVSG devices on the Tyenna River, Tasmania, Australia, and on the Paterson River, NSW, Australia. One point in time recorded from Tyenna River, Tasmania, Australia, in the middle of the observed water level range was also used for assessment of the optical methods relative to the available reference data. In total, 18 recorded points in time spanning the observed water level range were evaluated between the discharge estimates of the optical methods at Tyenna River, Tasmania, Australia. Furthermore, both the Tyenna River and Paterson River CVSG deployments were evaluated with long-term operational considerations for the implementation of CVSG methods into routine stream gauging. Table 1 provides a summary of the available reference data for the field case study sites presented in this work, as well as the measurement ranges observed.

2.6.1   Castor River, Ontario, Canada

The surface velocity profiles and discharge estimates for the Castor River case study site at Russell in Ontario, Canada, orientated facing across the stream from the left bank were analysed in this work utilising the published benchmark data (Perks et al., 2020b) from 10 April 2019, where an approximately 20 Hz 30 s duration video recording was captured at 15:55 local time (LT) (2688 × 1520 pixel resolution). The benchmark data included a reference Teledyne RDI Stream-Pro ADCP (Thousand Oaks, CA, USA) moving-boat transect with 0.05 m vertical cell resolution and the topmost cell measuring at 0.17 m depth. From the cross-sectional depth characteristics, the surface velocities extrapolated from the ADCP transect were scaled using the same 0.8 ratio assumed to approximate the depth-averaged velocity in the surface velocimetry approaches and then integrated across the channel cross section to estimate a comparable reference discharge. However, the most recently published gauging station rating was ultimately used as the reference discharge estimation, as this is currently the reported discharge that is estimated when the water level (3.77 m) is measured by the gauging station. This benchmark case study presents a favourably diffusely lit environment with visible surface rippling features across the full width of the cross section and a water surface reflective of the sky and vegetation. There are 12 ground control reference points provided with the recording for spatial rectification and scaling of pixel displacements over time. The cross section recorded by the moving-boat ADCP transect was used for the estimation of discharge and boundary distance factor surface velocity profile model fitting with an approximate maximum depth of 1.2 m over a 27 m-wide cross section (average depth of 0.8 m). Surface velocity analysis regions for all technologies utilised were conducted in a similar region across the downstream side of the ground control reference points closest to the bridge to the left of frame. To consider the variation resulting from different recording durations, raw CVSG surface velocities were analysed over the cross section for recording durations of 5, 10, and 20 s.

2.6.2   Irrigation channel, NSW, Australia

Canal channels are an important waterway type globally for the measurement of discharge, with countries such as the United Kingdom containing over 600 000 km of channels and ditches, while streams and rivers comprise some 270 000 km (Peacock et al., 2021). A field case study was undertaken with a camera oriented facing downstream from a hydraulic sluice gate control structure in an irrigation channel in NSW, Australia, on 10 September 2020 at 14:00 LT. A 30 Hz 30 s video recording (3840 × 2160 pixel resolution) formed the basis for the surface velocimetry estimations, with a reference measurement provided by a series of four SonTek RS5 moving-boat ADCP (San Diego, CA, USA) transects taken between 15 to 20 m downstream of the hydraulic control

Table 1. Field case study sites summary (water level ranges presented relative to local datums).

Site	Period	Distance to stream (m)	Water levels (m)	Reference gaugings	Ground control reference points
Castor River, Ontario, Canada	30 s	–	3.77	1 concurrent (2019)	12
Irrigation channel, NSW, Australia	30 s	–	135.80	1 concurrent (2020)	10
Tyenna River, Tasmania, Australia	56 d	5.9–7.3	0.31–0.87	344 historical (1964–2022)	9
Paterson River, NSW, Australia	122 d	0–22.5	0.78–10.54	157 historical (1987–2021)	0

structure within a time span of 8 min and a maximum discharge estimation difference of 8.5 % to the most outlying transect measurement. A non-uniform flow distribution is evident across the width and length of the irrigation channel with evidence of standing waves at the free surface including shimmering sun glare reflections. The area of the irrigation channel was surveyed with 10 ground control reference points for rectification of the image spatial scales and surface velocities from the pixel displacements over time. The cross section used for discharge estimation was taken from the ADCP reference transects with a maximum depth of 1.3 m and a transect width of 6.8 m. CVSG optical flow analysis along the length of the channel showed a marked reduction in flow visibility towards the region of the reference ADCP transects downstream (Fig. S1). Furthermore, the optical surface velocity measurement technologies were optimised to their suitable regions of interest. Hydro-STIV required a suboptimal analysis region closer to the camera and hydraulic structure in order to estimate one-dimensional space–time image stack angles for the determination of velocities, necessitating search line lengths which were unsuitably short for analysis under these conditions. Additionally for this case study, the CVSG analysis region was limited to 1 m channel section lengths, as the assumptions for CVSG analysis were found to be violated for sufficiently large analysis regions along the length of the cross section where the streamlines were not continuous. Beyond this, the CVSG raw surface velocities using recording durations of 5, 10, and 20 s have been analysed to assess the difference in measurements over differing sampling durations.

2.6.3 Tyenna River, Tasmania, Australia

The first long-term CVSG device field site was installed at the Tasmanian Government gauging station site at Newbury on Tyenna River, Tasmania, Australia, with CVSG analysis beginning from 5 March 2021 at 16:47 LT. A 216 km^2 catchment upstream provides continuous flow through the site with observed water levels between 0.26 and 0.87 m (maximum depths between 0.68 and 1.29 m) during CVSG operation. Along with a cross section of the site's bathymetry, nine ground control reference points were surveyed in the field of view of the camera in order to carry out reference analyses with DischargeLab and Hydro-STIV, while none were used for the CVSG analysis. The bed of the stream becomes visible at low water levels (< 0.4 m) with very little visibility of the water surface. Whilst the site experiences significant variations in lighting and flow conditions, the site's streamflow conditions are considered well-suited for remote optical measurement of surface velocities due to naturally occurring coverage of surface features above baseflow. However, it should be noted that the onset of standing waves was evident at the upper end of the range recorded by the CVSG device.

The CVSG device was mounted at an approximate water level of 6.32 m at a distance from the near-bank water edge, which ranged between 5.9 to 7.3 m over the recorded water level range. Video recordings were generally set to be taken with durations ranging between 5 to 20 s at 10 min intervals generally with a resolution of 1920 × 1080. The system was offline for 5 months between May and October 2021 during the first 12 months of operation included in this study. The CVSG analysis was configured to consider a constant 9 m long analysis region along the length of the stream with the positive flow direction provided to the right of the camera. A standard point cloud average temporal variation tolerance of 0.1 m was also set.

Historical manual discharge gauging measurements were provided for the site since 1964, averaging between 2 to 9 gaugings per year each decade over a water level range from 0.23 to 1.54 m, with the peak number of gaugings in the 1980s. There were 18 reference comparison time points selected from the CVSG recordings in March and April 2021 covering the range of water levels with a variety of lighting conditions. One of these comparison time points (30 March 2021, 12:12 LT, at a water level of 0.509 m) was used for the more detailed comparison of the estimated surface velocity profiles between the technologies. The most recent manual gauging measurement recorded within 0.05 m of the time point of the more detailed comparison time point's water level was also used for reference. This manual gauging measurement was undertaken on 7 August 2019 at 11:32 LT using a SonTek M9 RiverSurveyor moving-boat ADCP setup (San Diego, CA, USA) on the fixed cableway existing at the site.

2.6.4 Paterson River, New South Wales, Australia

A second long-term CVSG device field site was installed at the WaterNSW gauging station at Gostwyck on Paterson River, with analysis beginning from 3 November 2021

05:59 LT and finishing after being submerged on 4 March 2022. Significant flows with stream rises greater than 10 m that are ephemeral in nature at this site are more representative of regional Australian rivers. With a catchment area of 956 km^2 which is largely cleared for agricultural land use, 2 km upstream from the site is a confluence with the Allyn River, and Lostock Dam is 80 km upstream. Over the 4 months of CVSG operation at this site, water levels between 0.78 and 10.54 m were recorded (maximum depths ranging between 1 and 11 m), with cascading erosion of the far bank captured by the CVSG device at water levels higher than baseflow. Strong winds along the streamflow direction were observed in the first month of deployment significantly biasing low-flow surface velocities.

The CVSG device was installed perpendicular to the streamflow at an approximate water level of 11.34 m at a distance from the near bank water edge which ranged between 0 and 22.4 m over the recorded water level range. A cross section of the bathymetry was surveyed in a straight line along the same streamflow perpendicular axis as the camera orientation up to a water level of 8.38 m (2.2 m below the highest observed water level during CVSG operation), noting the location of the camera along this cross-sectional survey line. No ground control reference points were surveyed at this site, and there was therefore no comparison to other optical surface velocimetry technologies available. While alternative measurements for direct comparisons were not available, the latest published discharge rating estimates as well as the 157 historical manual gauging measurements taken across water levels ranging from 0.56 to 10.54 m since 1987 were used for reference. Dynamically varying downstream and upstream analysis boundaries were defined entirely to the right-hand (upstream) side of the CVSG device. Below 2 m water level, the analysis region was set to an 18 m channel length, while water levels above 2 m were able to analyse an expanded 35 m long channel length. The video recordings taken at the site were 10 s duration at a resolution of 1920 × 1080 every 10 min.

3 Results

3.1 Optical surface velocimetry

The surface velocity and ADCP (0.17 m depth) profiles across the cross-sectional distance for the Castor River case study (Fig. 3a) measured velocities increasing from the bank up to 1.5 m s^{-1} occurring by approximately 2 m across the channel for all measurement technology approaches. Within the midsection of the channel, velocities were measured between 1.5 and 2 m s^{-1}, with Hydro-STIV observing the lowest peak velocity, less than the peak measurement of the ADCP beneath the surface (which recorded some velocities on the order of 2 m s^{-1}). The lower resolution of Hydro-STIV search line measurements across the channel could be attributed to this result missing the peak velocities measured by the other technologies; however the other reference technologies consistently estimated higher velocities across the entire channel midsection. On the other hand, Hydro-STIV showed the highest rate of full velocity development from the edge of the channel, with the raw CVSG surface velocities estimating the lowest rate of full velocity development from the edge of the channel. Furthermore, the raw Discharge-Lab and CVSG velocity estimates tracked closely across the channel, although the optically estimated surface velocities were all in agreement with peak surface velocities occurring approximately 2 m closer to the left bank of the channel relative to the peak velocities measured by the ADCP. It can be seen that the optical surface velocity measurement technologies were able to measure velocities in the shallower regions closer to the channel edges than was possible with ADCP moving-boat transects.

With the application of the CVSG surface velocity profile model fitting methodology to all three optical surface velocity estimation approaches (Fig. S2a), it can be seen that whilst the raw surface velocity estimates largely fit within the bounds of the ADCP measurements at 0.17 m depth over the scale of the boundary distance factor, the resulting surface velocity profile model fits from each technology takes on a different shape. However, despite these differences in fitted surface velocity model profiles with the free stream surface velocities fitted ranging from 1.55 m s^{-1} in the case of Hydro-STIV, up to 1.9 m s^{-1} in the case of CVSG, as well as differences in the cross-sectional variable ranging between 0.45 (for CVSG) and 1.7 (for Hydro-STIV), the resulting discharges between all reference comparisons (including varying recording duration for raw CVSG analysis between 5 and 20 s and the ADCP discharge estimation using constant extrapolation to surface velocity) were within 5 % of the latest published gauging station rating discharge at the recorded water level (Table 2). For this case study, there was little sensitivity observed between the different measurement technologies, the duration of recording, or the resulting fitted surface velocity profile model parameters on the estimated discharges. Overall, the surface velocity profile model fitting methodology did not negatively impact the calculation of discharge for any of the surface velocity estimation technologies in this case study.

In the irrigation channel case study, the raw surface velocity profiles estimated were broadly in agreement about the shape of the velocity profiles across the channel (Fig. 3b), with the largest peak occurring within 2 m of the left bank, as well as reduced surface velocities measured in the middle of the channel and increased velocities towards the right bank. These velocity profiles are consistent evidence of the influence of the two hydraulic control gates upstream releasing water into the channel. Whilst the surface velocity magnitudes measured by the raw CVSG analyses from durations of 5, 10, and 20 s across the channel profile were more consistent with the ADCP-measured velocities at 0.13
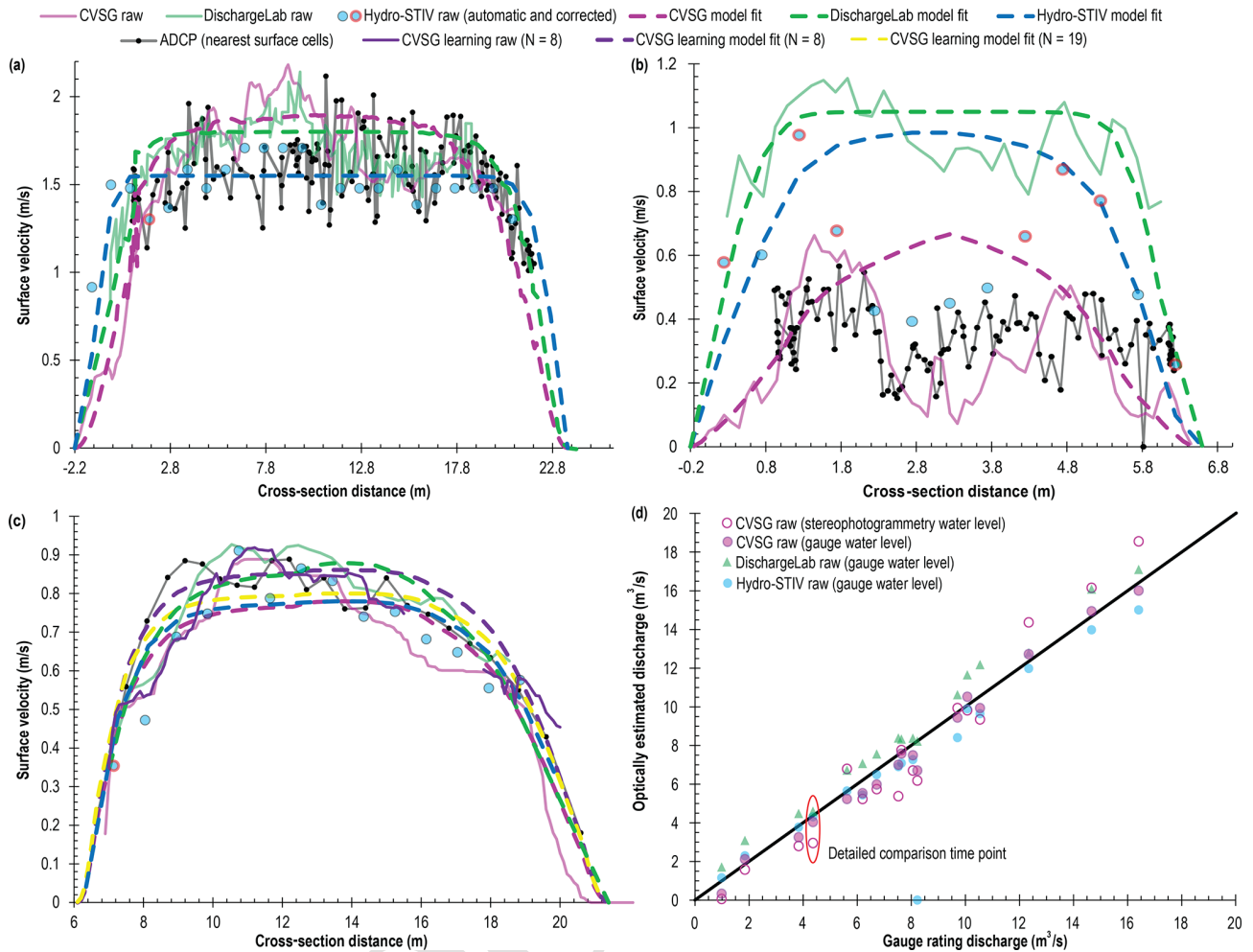
Figure 3. Detailed time point comparison of raw and model fitted velocity measurements plotted with nearest surface ADCP measurement cells over the cross sections at **(a)** Castor River, Ontario, Canada; **(b)** an irrigation channel in NSW, Australia; and **(c)** Tyenna River, Tasmania, Australia. **(d)** Correlation plot between the gauge rating and optically estimated discharges at comparison time points at Tyenna River, Tasmania, Australia, with the detailed comparison time point indicated. CVSG 5 s duration surface velocities shown for **(a)** Castor River, Ontario and **(b)** the irrigation channel in NSW, Australia. CVSG 10 s duration surface velocities shown for **(c, d)** Tyenna River, Tasmania, Australia. Hydro-STIV velocity estimates outlined in black were automatically produced, whereas the estimates outlined in red were corrected to the Fourier result or manually corrected to reduce automatically overestimated velocities resulting from the higher-frequency surface wave patterns or underestimated tracer-poor search lines. TS4

to 0.19 m depth, the surface velocities estimated by Hydro-STIV and DischargeLab were on the order of double within 2 m of the channel edges. While the objective truth of the surface velocity profile across the channel is not known, the Hydro-STIV analysis contains results with unclear space–time pattern angle identification under these conditions. It is important to note the irrigation channel site differs substantially from other trial sites with a downstream field of view and highly turbulent flow conditions discharged through an engineered channel. Furthermore, this case study not only demonstrates where site selection can lead to troubling optical surface velocity measurements, but also highlights a case where the assumptions of the CVSG surface velocity profile model are not valid and therefore should not be applied (as in

Fig. S2b). Although the discharge is only inferred from the signals measured by the reference technologies, only the raw CVSG measurements and ADCP discharge estimates agree within 5 % across all recording durations analysed (Table 3).

With 133 samples measured over the length of the ADCP cross section, the resulting ADCP measurement resolution was on the order of 0.04 m per sample (with 1 s per sample). This meant that the ADCP sampling durations for each segment of the channel was on the order of 2.5 s per 0.1 m channel cross-sectional segment. The lowest duration CVSG optical surface velocity analysis occurred over 5 s sampling the entire cross section simultaneously at 0.1 m resolution (not possible with a moving-boat ADCP transect), which resulted in a 1 % to 4 % difference to the ADCP discharge es-

Table 2. Summary of discharge estimates for gauging technologies at Castor River, Ontario, Canada (10 April 2019, 15:55 LT).

Measurement	Type	Duration	Discharge ($m^3 s^{-1}$)
Water level	Published rating at 3.77 m	–	27.8
ADCP (surface)	Constant extrapolation to surface	NA	(+1 %) 28.2
CVSG	Raw	5 s	(−2 %) 27.3
	Raw	10 s	(−4 %) 26.8
	Raw	20 s	(−4 %) 26.6
	Model fit ($v_\infty = 1.9$, $b = 0.45$)	5 s	(+1 %) 28.1
DischargeLab	Raw	25 s	(+4 %) 28.9
	Model fit ($v_\infty = 1.8$, $b = 0.8$)	25 s	(+3 %) 28.6
Hydro-STIV	Raw	25 s	(+1 %) 28.0
	Model fit ($v_\infty = 1.55$, $b = 1.7$)	25 s	(+2 %) 28.3

NA = not available

Table 3. Summary of discharge estimates for gauging technologies at an irrigation channel in NSW, Australia (10 September 2020, 14:00 LT).

Measurement	Type	Duration	Discharge ($m^3 s^{-1}$)
ADCP (profile)	Moving boat	124 s	1.65
CVSG	Raw	5 s	(+2 %) 1.68
	Raw	10 s	(−1 %) 1.64
	Raw	20 s	(−4 %) 1.58
	Model fit ($v_\infty = 0.8$, $b = 0.4$)	5 s	(+55 %) 2.56
DischargeLab	Raw	20 s	(+215 %) 5.19
	Model fit ($v_\infty = 1.05$, $b = 2.5$)	20 s	(+224 %) 5.34
Hydro-STIV	Raw	20 s	(+111 %) 3.48
	Model fit ($v_\infty = 1$, $b = 1$)	20 s	(+189 %) 4.77

timate. However, the incorrect application of the surface velocity profile model resulted in estimates 55 % higher than the reference ADCP discharge estimate.

After 25 d into the operation of CVSG at the case study site on the Tyenna River capturing 2452 gaugings, the first flow event had been observed (reaching a maximum recorded water level of 0.735 m) with the water level receding to 0.509 m on 30 March 2021 at 12:12 LT; the comparison surface velocity profile estimates were found to be grouped within ± 0.1 m s^{-1} in the midsection of the channel (Fig. 3c). The ADCP-measured mean velocities across the channel were scaled up to estimate the surface velocity using the assumed ratio of 0.8 recorded at a water level 0.038 m higher on 7 August 2019 at 11:32 LT. Similarly, this resulted in ADCP-estimated surface velocities within the same range of variability measured by the surface velocimetry reference methods but with a 14 % higher calculated discharge relative to the latest published discharge rating at 0.509 m water level (Table 4). Although the true discharge is not known, all reference technologies estimated discharges within 10 % of the latest published discharge rating at this water level, except

for the ADCP profile recorded 601 d prior at a higher water level estimating within 15 %.

Surface velocity profile model fits for this case study measurement ranged between 0.78 (CVSG and Hydro-STIV) to 0.88 m s^{-1} (DischargeLab) for free stream velocities and 1 (DischargeLab) to 1.4 (Hydro-STIV) for cross-sectional variables (Fig. S2c). The model fitting of the raw surface velocities estimated across all optical measurement technologies was not found to have any negative measurable impacts on the calculation of discharge. However, in practice the model fit would not be computed using the raw velocities alone, as the CVSG system would instead compute the model fit of the learning velocity distribution after the 25 d of measurements that had resulted in eight observations within 0.005 m and an accumulated 72 % optical flow measurement coverage over the width of the cross section at this water level (Fig. S3a).

Furthermore, up to this measurement time there had been a total of 2452 CVSG gaugings across a wider range of water levels, and the resulting learning discharge rating was also estimated (Table 4). Additionally, quantifying any further change in the learning estimations considering a point in time which is another 30 d advanced into the CVSG gaug-

ings (Fig. S3b) saw the difference between the learning estimated CVSG discharges and the latest published discharge rating at 0.509 m water level drop from within 6 % to within 2 %. However, it is important to note that the variability in
5 CVSG discharge estimates is minimal compared to the variation in manual gauging estimates from similar water levels since 1989. This variation in discharge estimates over time is often a function of cross section changes and subsequent ratings shifts. Relative differences are expected to be within the
10 realm of uncertainty of the true discharge, particularly as the discharge has only been measured at this water level once in 1966, with measurements within 0.005 m occurring 5 times (most recently in 1989) and 37 measurements within 0.05 m (the two most recent occurring 2 and 8 years prior to the time
15 of this case study recording) (Fig. 4).

Further comparison of the reference optical surface velocimetry technologies at 16 time points along the time series recorded at Tyenna River shows the importance of discharge gauging technology assessments over multiple con-
20 ditions (Table 5). With the evaluation of more time points, an understanding of the most suitable conditions for gauging can be built from the statistics of the RMSE, mean percentage bias difference, and the NSE relative to the reference latest gauging station rating. In the absence of gauged wa-
25 ter levels, the raw CVSG discharge estimation had the greatest time series absolute error performance with an RMSE of 1.28 m^3 s^{-1} however suffered a worse bias in the mean difference relative to the latest gauging station discharge rating, with the learning estimations demonstrating improving
30 this bias to 1.9 % in hindsight after 12 months of learning with an increased 2.28 m^3 s^{-1} RMSE. For the CVSG discharge estimations using the gauge water level, the RMSEs were reduced to less than half of the stereophotogrammetry-estimated water-level-based discharge estimations, implying
35 that the stereophotogrammetry estimation of water level is the largest source of error in the discharge estimate.

3.2 Stereophotogrammetry water level detection

During the operation of the CVSG system on the Tyenna and Paterson rivers, water levels were remotely estimated using
40 stereophotogrammetry with every recording possible, requiring sufficient daylight, as night vision equipment was not installed at these sites during the period of this evaluation. The time series of remotely estimated water levels were classified into different error ranges relative to the water levels
45 recorded by the reference gauging stations at Tyenna River (Fig. S4a) and Paterson River (Fig. S4b). Water level estimation errors within 0.005 m were considered to be exactly correct relative to the 0.01 m water level database precision used in CVSG operation in this work. Errors found to be within
50 0.05 m were also expected to be useful, as this is the water level Savitzky–Golay filter window size used in the CVSG learning distributions of these studies. Both sites in this study with CVSG deployed suffered from higher variability during

lower flows, corresponding to low visual distinction of the texture of the water surface, particularly with the greater dis-
55 tance of the site to the edge of the Paterson River at low flows and clear water displaying the bed of the Tyenna River.

Correlation plots between the gauge water level and the CVSG stereophotogrammetry-estimated water level at Tyenna River (Fig. 5a) and Paterson River (Fig. 5b) show the
60 remotely estimated water levels compared over the range of the gauge recorded water levels with some potential clustering of different error regions at particular water levels. From this, the cumulative error distributions (Fig. 5c) shows 2 % and 1 % of measurements taken over the study period were
65 considered to be precise at the Tyenna River and Paterson River sites, respectively. Furthermore, just 16 % and 7 % of measurements at the sites were considered within the CVSG learning distribution noise tolerance, with the remaining majority of measurements falling outside of this error range with
70 potentially significant contributions to discharge bias possible as a result.

3.3 Time series discharge

The real-time estimation of discharge over time relative to the latest gauging station rating at Tyenna River using CVSG
75 raw, learning model fit, and learning rating all demonstrated the ability to capture the patterns of hydrographic rises and falls despite the significant presence of errors in the remote stereophotogrammetry estimation of water level (Figs. 6a and S5a). Whilst the raw CVSG discharge estimates follow
80 the latest gauging station rating estimation more closely than the learning estimations, this can be attributed to the significantly higher vulnerability of the learning estimates for any individual time point to errors in the water level estimation. However, with the learning process continuing over
85 12 months at the site, a marked improvement in the discharge estimation from the learned discharge rating (despite the underlying water level estimation errors) was evident.

Using the gauge water level in the CVSG analysis independently parallel to the stereophotogrammetry-estimated
90 measurements yielded learning discharge estimations rapidly improving on the variability observed in the raw CVSG measurements (which are each independently estimated through time) relying on the suitability of the naturally occurring conditions for optical flow at the time of measurement (Figs. 6b
95 and S5b). Even though the true discharges at the measurement times are not known, the CVSG learning discharge estimations using the gauge water levels at the time overestimated the discharges of events occurring in April 2021 relative to the latest gauging station discharge rating by up to
100 20 %. However, the application of the learning CVSG discharge rating after 12 months in hindsight demonstrated a stronger agreement to the gauging station rating in this series of events. While the original learning estimate may have been correct at the time of the measurement, with non-stationary
105 site conditions resulting in a shift in the true discharge rating

Table 4. Summary of discharge estimates for gauging technologies at Tyenna River, Tasmania, Australia (30 March 2021, 12:12 LT) using gauge water levels.

Measurement	Type	Duration	Discharge (m^3 s^{-1})
Water level	Published rating at 0.509 m	–	4.37
ADCP (profile)	Moving boat 7 August 2019, 11:32 LT, at 0.547 m	1522 s	(+14 %) 4.97
CVSG	Raw	10 s	(−6 %) 4.09
	Model fit ($v_\infty = 0.78$, $b = 1.2$)	10 s	(−6 %) 4.11
25 d gauged	Learning model fit ($v_\infty = 0.86$, $b = 1.39$) – 8 observations at 72 % coverage	10 s	(+6 %) 4.63
	Learning rating (2452 observations)	–	(+5 %) 4.58
55 d gauged	Learning model fit ($v_\infty = 0.8$, $b = 1.47$) – 19 observations at 84 % coverage	5 s	(−1 %) 4.33
	Learning rating (3890 observations)	–	(+2 %) 4.46
DischargeLab	Raw	10 s	(+5 %) 4.59
	Model fit ($v_\infty = 0.88$, $b = 1$)	10 s	(+4 %) 4.55
Hydro-STIV	Raw	10 s	(−8 %) 4.03
	Model fit ($v_\infty = 0.78$, $b = 1.4$)	10 s	(−3 %) 4.23
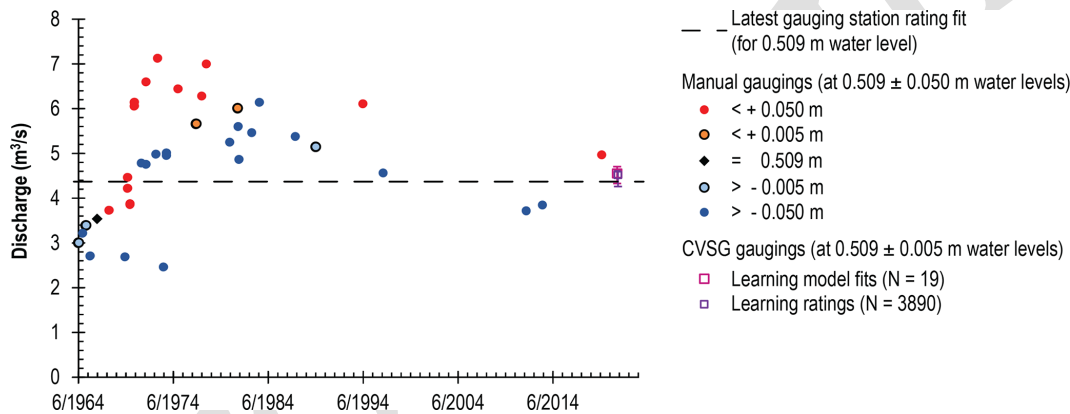
Figure 4. Historical and CVSG gaugings at Tyenna River, Tasmania, Australia, in the vicinity of 0.509 m water level.

after a further 10 months of site evolution, it is considered more likely that the lower agreement between the real-time CVSG learning discharge estimations and the latest gauge discharge rating was due to discontinuities from the sparser CVSG device sampling during this period beyond the range of previously recorded measurements.

The Paterson River site demonstrated more challenging conditions for continuous optical measurements of surface velocities due to surface texture combined with CVSG device distance to the water surface at low flows and the wider channel cross section approaching the eye level of the camera at the higher observed flow events. The resulting CVSG discharge estimations at Paterson River (Figs. 6c, S7a, 6d, and S7b) demonstrate the utility of the learning model fit and discharge rating for improving the operational gauging capability using optically measured surface velocities.

Similarly to the findings at Tyenna River, the difference between the CVSG learning results relative to the latest gaug-

ing station discharge rating at Paterson River implied the majority of discharge gauging noise was the result of noise in the stereophotogrammetry-estimated water level (Fig. S8a). This noise, as evidenced by the distribution of CVSG water level error (Fig. 5c), was significantly worse at Paterson River during low flows approaching the upper range of the point cloud distance to reach the near bank intersection with the water surface. Despite this significant noise, the CVSG learning discharge estimations demonstrated a capability to reduce this influence of this error both in real-time learning and improve further with more measurements. Interestingly, the magnitude of raw CVSG discharge estimation errors was remarkably similar between the remotely sensed and gauge water level cases due to the most significant errors in the raw measurements occurring during flow events with poor surface velocity visibility. In these cases, the learning surface velocity distribution fitted model demonstrated significant improvements to the raw optical measurements. Further

Table 5. Summary of comparison time points relative to the gauge rating at Tyenna River, Tasmania, Australia.

Measurement	Type	RMSE ($m^3\,s^{-1}$)	NSE
CVSG (stereophotogrammetry-estimated water level)	Raw	1.28	0.905
	Learning model fit	2.69	0.581
	Learning rating	2.26	0.705
	Learning rating (12 months)	2.28	0.719
CVSG (gauge water level)	Raw	0.48	0.986
	Learning model fit	1.18	0.919
	Learning rating	1.03	0.939
	Learning rating (12 months)	0.60	0.979
DischargeLab (gauge water level)	Raw	0.97	0.945
Hydro-STIV (gauge water level)	Raw	0.68	0.973
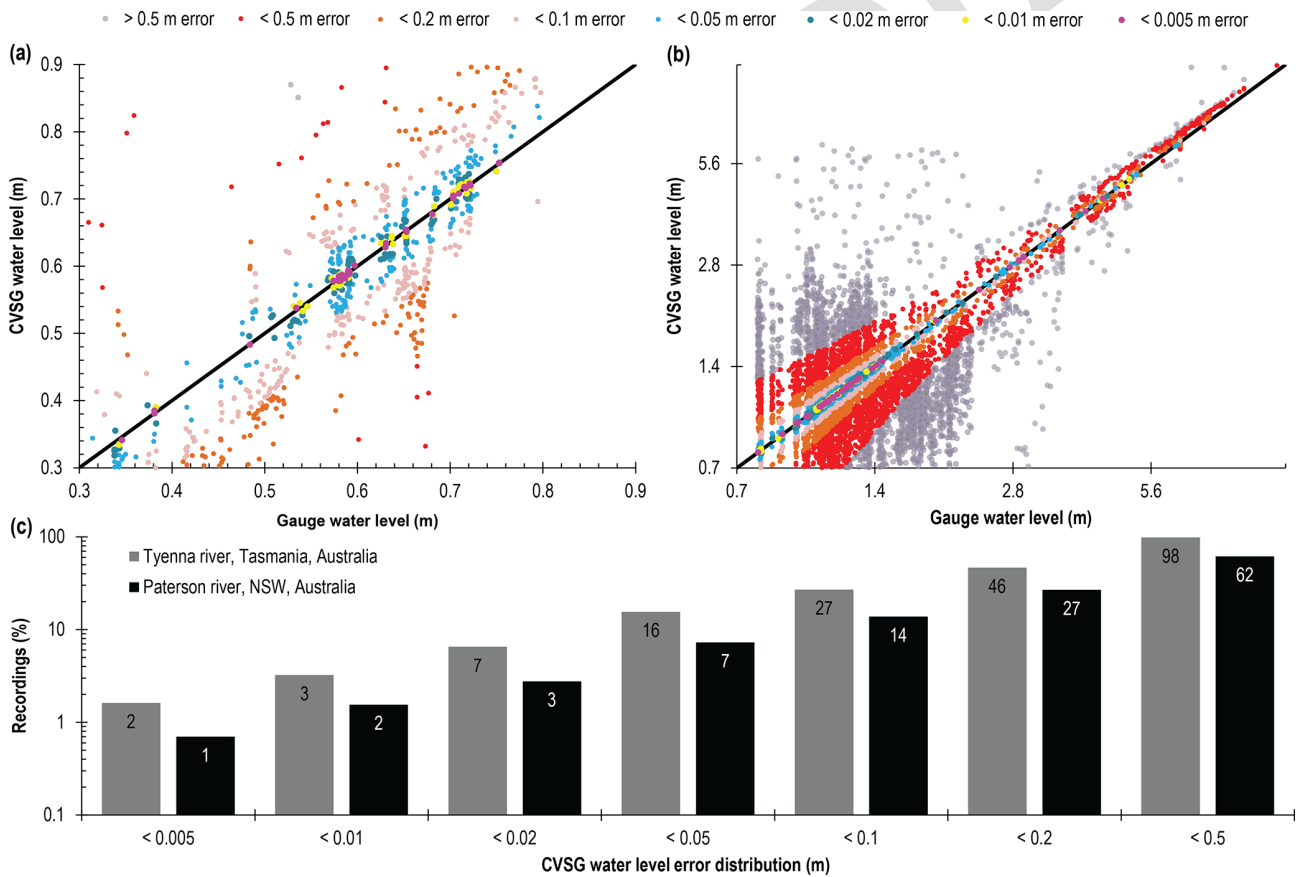
Figure 5. Correlation between gauge- and stereophotogrammetry-estimated CVSG water level classified according to error magnitude at **(a)** Tyenna River, Tasmania, Australia, and **(b)** Paterson River, NSW, Australia, on a logarithmic scale. The cumulative stereophotogrammetry-estimated CVSG water level error class distribution **(c)** for both Tyenna River, Tasmania, Australia, and Paterson River, NSW, Australia, on a logarithmic scale.
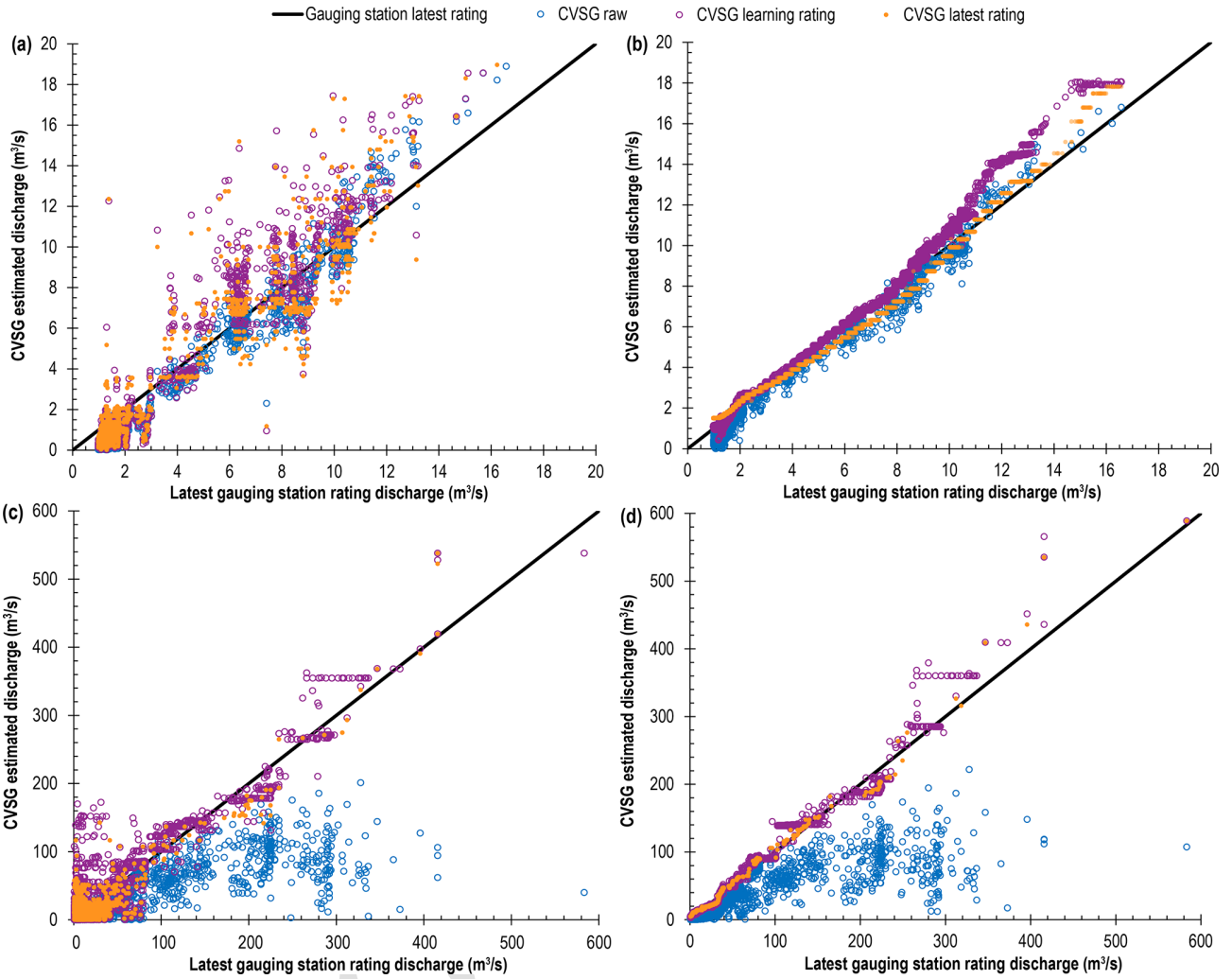
Figure 6. Correlation plots for the latest gauging station rating discharge time series against the CVSG-estimated discharge time series at Tyenna River, Tasmania, Australia, using **(a)** stereophotogrammetry-estimated water levels and **(b)** gauge water levels, as well as at Paterson River, NSW, Australia, using **(c)** stereophotogrammetry-estimated water levels and **(d)** gauge water levels.

to this, the reduced water level estimation noise when using the gauge water level (Fig. S8b) displayed significantly reduced error in the CVSG learning discharge estimations converging much faster between the real-time and 4-month hindsight rating estimates.

3.4 Adaptive learning discharge rating

The latest CVSG learning discharge ratings after 12 months of deployment at Tyenna River using the stereophotogrammetry-estimated water levels and gauge water levels were found to be within the range of historical manual gaugings (Fig. 7). With the manual gaugings classified by decade, it is important to understand the foundation of the measurements behind the latest gauging station discharge ratings, as well as how the degree of fit to the smooth gauging station rating curves. Whilst the majority

of the CVSG learning rating using stereophotogrammetry-estimated water levels was found to be within the range of the 344 manual gaugings undertaken at the Tyenna River site since the 1960s, the discharge ratings for stereophotogrammetry-estimated water levels below 0.4 m (where water clarity impacted measurements) demonstrated a bias to higher discharge. There was also a transition point from high discharge estimates to low discharge estimates using the stereophotogrammetry-estimated water levels in the vicinity of 0.6 m. Furthermore, the CVSG learning discharge rating using gauge water levels demonstrated a tighter convergence to the most recent manual gaugings and the latest gauging station rating.

It is important to note the upper range of discharge measurements above 0.79 m gauged by the CVSG system to 0.87 m has not been manually gauged at Tyenna River for more than 10 years, where the RMSE to the latest gauging
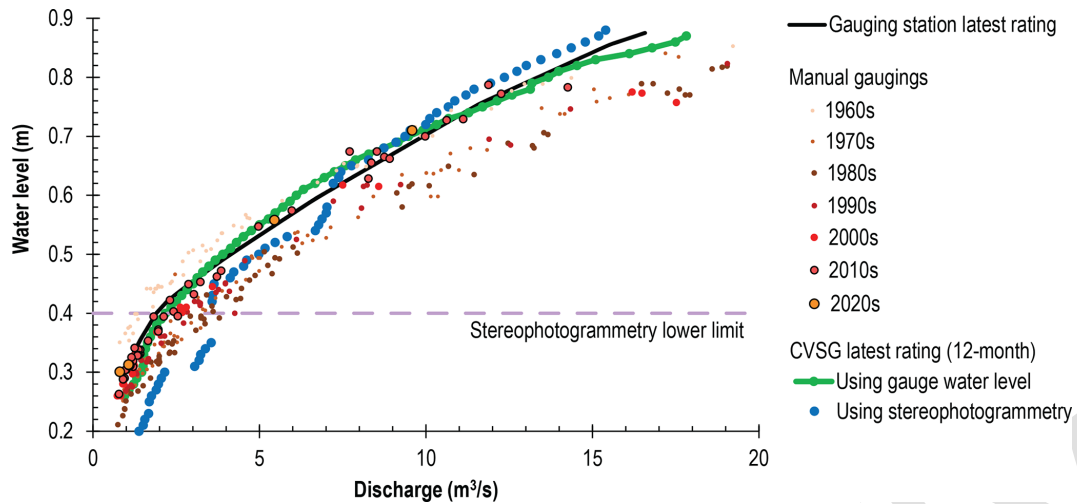
Figure 7. Discharge gaugings at Tyenna River, Tasmania, Australia, with CVSG learning ratings after 12 months of deployment using stereophotogrammetry-estimated water levels and gauge water levels.

station discharge rating is above $2\,\mathrm{m}^3\,\mathrm{s}^{-1}$ with mean differences greater than 20 % (Table 6). All real-time CVSG discharge estimations over the time series demonstrated less RMSE than the most recent decade containing an increased manual gauging range that includes the range measured by the CVSG system. For the stereophotogrammetry-estimated water-level-based CVSG discharge ratings, the RMSE showed an increasing trend with the progression of the learning process primarily due to an increasing gauged water level range containing sparse observations with more absolute discharge error. However, the NSE of these learning CVSG discharge ratings showed increasing skill relative to the latest gauging station discharge rating. The CVSG discharge estimations using the gauge water level demonstrated a relatively stable fit to the reference discharge rating, while the learning method was able to provide a significant reduction in the mean difference to the reference discharge rating.

After 4 months of CVSG operation at Paterson River, the system had gauged the maximum water level range that had been manually gauged since as far back as the 1980s, with the CVSG discharge estimations using the gauge water level producing an estimated discharge at the top of this range within 0.22 % of the discharge measured in the 2000s at this water level. Whilst the manually gauged discharges at the upper recorded water levels appear to be sparsely measured, the CVSG discharge learnings using either gauge water levels or stereophotogrammetry-estimated water levels were in agreement with the manual gaugings across the measurement range (Fig. 8). Further to this, the shape of the CVSG discharge ratings agrees more closely with the shape of the rating curve implied by the manual gaugings, rather than the smoother fit of the gauging station rating curve.

The summary statistics of the CVSG discharge estimations at Paterson River (Table 7) showed that the learning CVSG

analysis using stereophotogrammetry-estimated water levels were significantly impacted by the error in the water level estimation resulting in mean differences in excess of 100 % relative to the reference latest gauging station discharge rating. However, the NSEs of the learning discharge estimations were significantly higher than the raw CVSG discharge estimations.

3.5 Overview of results

The results of this work found broadly comparable gauging results using the raw data of the different measurement technology approaches employed, predominantly falling within a relative error of 15 % under suitable conditions when comparing between the results of both the detailed surface velocity distribution case studies and longer deployment timescales evaluated. However, it was demonstrated that the use of a surface velocity profile model fitted to raw measurements under suboptimal or only partially measurable conditions could be beneficial to improving the reliability of surface velocimetry methods. Furthermore, the learning of an adaptive surface velocity distribution extended to an adaptive learning discharge rating produced robust results for stream gauging over time. While the initial CVSG results for the non-contact measurement of water levels using stereophotogrammetry found less than 20 % of measurements within 0.05 m, the learning capability of the CVSG approach presented was able to converge towards a robust discharge rating despite noisy raw observation data.

4 Discussion

The study has outlined a new non-contact optical stream gauging approach (CVSG) and provided a detailed compara-

Table 6. Summary of site gauging results for Tyenna River, Tasmania, Australia relative to the latest gauging station discharge rating.

Measurement	Type	N	Range (m)	RMSE ($m^3 s^{-1}$)	NSE
Manual gaugings	1960s	57	0.35–1.21	1.11	0.964
	1970s	82	0.25–1.33	2.79	0.916
	1980s	90	0.23–1.51	3.23	0.884
	1990s	43	0.27–1.54	2.58	0.936
	2000s	25	0.26–1.40	2.18	0.823
	2010s	42	0.26–0.79	0.38	0.989
	2020s	5	0.30–0.71	0.32	0.990
CVSG (stereophotogrammetry-estimated water level)	Raw (time series)	2133	−0.33–1.05	1.05	0.904
	Learning model fit (time series)	2232	−0.33–1.05	1.54	0.793
	Learning rating (time series)	2232	−0.33–1.05	1.50	0.805
	Learning rating (1 month)	1795	−0.33–0.79	1.28	0.891
	Learning rating (2 months)	2133	−0.33–1.05	2.02	0.922
	Learning rating (12 months)	17 178	−0.33–1.07	2.54	0.956
CVSG (gauge water level)	Raw (time series)	2141	0.31–0.87	0.63	0.961
	Learning model fit (time series)	9049	0.31–0.87	0.56	0.976
	Learning rating (time series)	9293	0.31–0.87	0.53	0.979
	Learning rating (1 month)	3276	0.31–0.73	0.26	0.993
	Learning rating (2 months)	3905	0.31–0.87	0.90	0.955
	Learning rating (12 months)	19 005	0.26–0.87	0.60	0.983
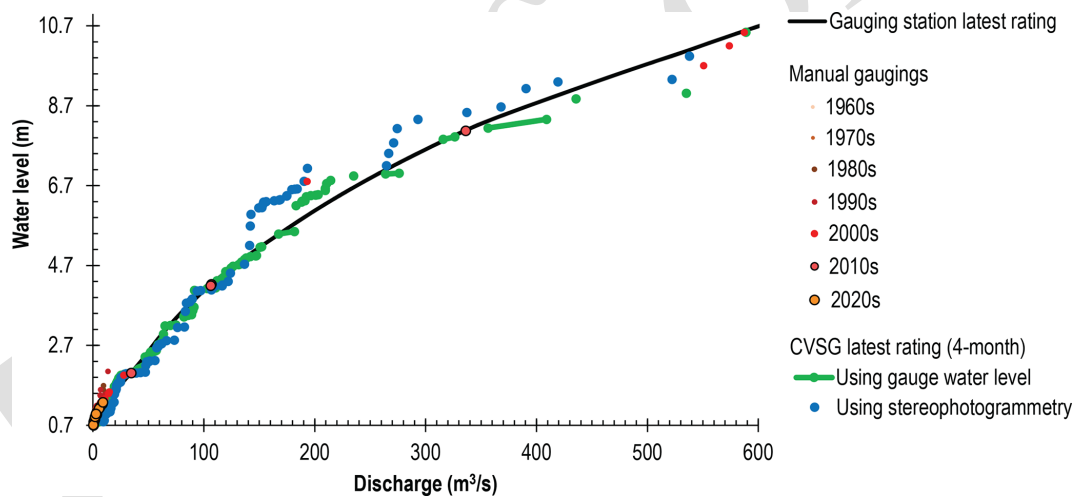
Figure 8. Discharge gaugings at Paterson River, NSW, Australia, with CVSG learning ratings after 4 months of deployment using stereophotogrammetry-estimated water levels and gauge water levels.

tive analysis against existing optical approaches (Discharge-Lab and Hydro-STIV) and the current standard technologies and historical measurements informing gauging stations. Results highlight that the advancements in stereophotogrammetry and machine learning approaches can overcome some of the challenges of non-contact optical stream gauging and provide insights into the added value of these emerging operational technologies. Whilst a significant uncertainty on the order of 6 % has been found to be possible from user variations in ADCP discharge estimations (Despax et al., 2019), as well as comparable deviations evident in a study of ADCP

measurement validation (Oberg and Mueller, 2007), a similar order of magnitude in difference between direct technology comparisons was found in all but one exceptional case in an irrigation channel in NSW, Australia. A study in an irrigation canal using an experimental video camera system with LSPIV and optical water level detection on a staff gauge demonstrated results within 5 % of the reference estimates but highlighted that reflections and shadows produced negative effects on the detection of motion, requiring further consideration of spatial filters and light distribution (Lee et al., 2010).

Table 7. Summary of site gauging results for Paterson River, NSW, Australia relative to the latest gauging station discharge rating.

Measurement	Type	N	Range (m)	RMSE ($m^3 s^{-1}$)	NSE
Manual gaugings	1980s	17	0.81–1.69	4.45	0.455
	1990s	45	0.66–2.04	4.51	0.540
	2000s	50	0.56–10.54	29.42	0.917
	2010s	38	0.61–8.07	6.20	0.908
	2020s	7	0.71–1.28	0.24	0.993
CVSG (stereophotogrammetry-estimated water level)	Raw (time series)	6228	−0.2-1-9.94	21.92	0.680
	Learning model fit (time series)	6246	−0.21–9.94	16.13	0.827
	Learning rating (time series)	6246	−0.21–9.94	15.86	0.832
	Learning rating (1 month)	1940	−0.14–8.13	17.74	0.953
	Learning rating (2 months)	3534	−0.19–8.13	20.83	0.939
	Learning rating (4 months)	6265	−0.21–9.94	25.18	0.950
CVSG (gauge water level)	Raw (time series)	6592	0.78–10.54	19.04	0.973
	Learning model fit (time series)	18 352	0.78–10.54	5.47	0.951
	Learning rating (time series)	18 624	0.78–10.54	4.89	0.961
	Learning rating (1 month)	1978	0.78–7.86	9.60	0.981
	Learning rating (2 months)	3627	0.78–7.86	8.95	0.982
	Learning rating (4 months)	6627	0.78–10.54	20.78	0.942

There has been some LSPIV discharge uncertainty estimations undertaken from recordings of a stream in the French Alps (Dramais et al., 2011) showing less than 2 % discharge deviation for recording durations more than 4 s, consistent with the CVSG results tested using different durations. Within situ profile measurements, this study in the French Alps found the uncertainty in the mean velocity coefficient to be close to 7 %, with the largest source of uncertainty up to 15 % possible without velocity depth profile measurements within the flow range of interest. Further to this, the sensitivity analysis of this French Alps study examined the effect of waves (negligible), cross-sectional transects (±4 %), and water level errors at 4 % from a 10 cm error (noting that the CVSG stereophotogrammetry water level error was within this range only 27 % and 14 % of the time at the Tyenna River and Paterson River sites, respectively). Alternative methods for estimating the uncertainty of stream discharge rating curves have been compared in Kiang et al. (2018), finding a wide variation in uncertainty estimates resulting from different methods, which demonstrated the necessary careful selection and communication of the assumptions of the uncertainty estimates provided.

By using UAV footage of artificially seeded low-flow conditions (average surface velocities between 0.12 to 0.14 m s^{-1}) on a river in Serbia, a significant sensitivity to algorithm parameters was apparent for LSPIV, large-scale particle tracking velocimetry (LSPTV), and optical tracking velocimetry (OTV) relative to the less sensitive SSIV (an enhancement of LSPIV) and Kanade–Lucas Tomasi image velocimetry (KLT-IV) (using an optical flow algorithm, similarly to CVSG) (Pearce et al., 2020). Whilst there has been some evidence that KLT optical flow performance degrades

in low lighting (Wang and Miao, 2010), the Farneback optical flow approach used by CVSG has been found to provide more robust results in comparison studies (Nemade and Gohokar, 2019; Shi et al., 2020). This identified sensitivity of algorithm parameters has been reinforced by simulations using LSPIV, showing substantial care must be taken for ensuring reliable results with regards to seeding shapes/sizes/densities, frame rates, recording durations, and camera angles (Hauet et al., 2008; Pumo et al., 2021). The general vulnerability of optical surface velocimetry methods to measurement setup (Detert, 2021) and environmental conditions, such as evidenced by a study of varying rainfall intensity particularly finding LSPIV-based autocorrelation methods to be susceptible to biased results under higher rainfall intensities (whilst results were demonstrably improved by sufficiently low rainfall intensities) (Naves et al., 2021), reinforces the need and utility of methodologies, such as those presented in this work, for increasing robustness to visual environmental noise pertaining to individual measurements.

The CVSG learning surface velocity distribution and discharge rating results evaluated in this study provide evidence to the benefits of the presented methods for improving measurement accuracy and reliability over time. Given increasing frequency of extreme rainfall yielding flow events that exceed manual gauging records (Steinbakk et al., 2016), the ability of the CVSG approach to learn and adapt over time is particularly valuable. Whilst the entire range of the discharge ratings developed and evaluated did not necessarily yet contain a sufficient combination of quantity and quality of observations, this is similarly evident in the best available estimates provided from the reference gauging station discharge rating fits (which may be overly smoothed due to lim-

ited temporal and vertical–spatial data density). With the persistent measurement of velocities, sudden or gradual changes in velocity distributions over time can be detected in order to identify when the resurveying of a site's bathymetry is necessary (Peña-Haro et al., 2021).

The results of this study between CVSG-estimated time series discharges and discharge ratings using stereophotogrammetry-estimated water levels and provided gauge water levels showcased the improvement in non-contact measurements that could be possible with improvements to the remotely estimated water levels alone. A combination of optical approaches to water level estimation using water line detection spatio-temporal texture histograms (Eltner et al., 2018) or deep learning (Eltner et al., 2021), as well as grayscale brightness or motion segmentation (Peña-Haro et al., 2021) combined with a stereo camera approach has potential for reducing remotely estimated water level noise and improving the range of suitable operational environments. This concept could simultaneously reduce the uncertainties and site deployment barriers associated with ground control reference points (Le Coz et al., 2021). Significant work has been undertaken towards developing and applying photogrammetry techniques operating using different camera perspectives from more than one camera for long-term automated water level and discharge measurements (Stumpf et al., 2016). Stereo cameras have demonstrated potential added value to stream gauging applications (Ran et al., 2016; Li et al., 2019), with the CVSG system providing a reduction in the barrier to the deployment of a stereo camera-based optical stream gauging site. With continuous automated site resurveying with every video recording, the quantification of cross-sectional changes and vegetation growth offers significant advantages to monitoring streams without stationarity assumptions (Westerberg et al., 2011). A comprehensive study evaluating the use of stereo camera systems such as CVSG for quantifying adaptive cross sections is an important area of future research to be determined over studies spanning longer timescales with significant erosion and/or accretion events at suitable study sites.

Whilst optical-based non-contact stream gauging has well-documented advantages for gauging high-flow events compared to alternative methods (Le Coz et al., 2010), well-understood and relatively stable low-end discharge ratings could be provided to the CVSG system as a manually provided and updated basis for estimating low flows where low-flow site conditions may be unsuitable. However, the depictions of discharge ratings evaluated in this study are simplified one-dimensional water-level-dependent discharge estimates (as is commonly developed and applied for gauging station discharge ratings), but this is a simplification of the variation in discharge resulting from the changing hydraulic gradients across the rising and falling stages of hydrographs (Fenton, 2018). This nuance could be developed automatically through the significantly improved gauging data den-

sity offered by optical surface velocimetry approaches such as CVSG, providing an additional dimension for the generation of discharge ratings dependent on both water level and the hydraulic gradient.

While the CVSG system evaluated utilised Savitzky–Golay filtering, it is noted that recent improvements on this method have been developed addressing the known pitfalls of the technique (Schmid et al., 2022). Beyond the approaches in this study for optically discerning water surface motion, further enhancement of optical measurement capabilities could be achieved through novel techniques using well-studied and bounded principles of fluid dynamics (Khalid et al., 2019). An ensemble of surface velocimetry techniques could be applied, given sufficient computational power, to provide an additional quantification of algorithm-based uncertainty similar to ensemble approaches employed in other fields for quantifying model structural sensitivity (Nearing and Gupta, 2018) and facilitate the identification of disagreements between methods under particular sites and conditions over time while expanding the broader applicability of the technology through the advantages offered by each technique. Furthermore, the optical nature of the methods developed supposes the possibility for the incorporation of additional computer vision analysis through rainfall (Jiang et al., 2019; Chen et al., 2019; Wang et al., 2022), wind (Cardona, 2021), and water turbidity (Leeuw and Boss, 2018) monitoring.

5   Conclusions

This study has demonstrated the development of an automated operational optical stream gauging system employing methods providing improved reliability for remotely gauging streams using state-of-the-art surface velocimetry technologies across varying flow and lighting conditions. Evaluation of the existing best practice in available stream measurement technologies and published discharge ratings across the array of site conditions evident in this work demonstrated that the methods in this study were similarly effective for gauging stream discharge to existing accuracy benchmarks. This work did not address errors associated with cross-sectional area changes and the capability of the CVSG system to extract stereophotogrammetry-estimated elevations of the dry channel areas to inform changes to discharge ratings, which is recommended for future research using stereo imagery-based optical stream gauging approaches. In addition, the challenges associated with analysing surface velocity at night and quantifying water level through stereophotogrammetry under a range of lighting conditions and greater distances provide opportunities for future work. Despite these challenges, non-contact and automated solutions offer a significantly greater density of velocity-stage observations resulting in up-to-date adaptively learning discharge ratings through time. As climate-driven extreme weather events in-

crease in frequency, it is increasingly important to develop and apply flexible monitoring tools, such as CVSG, that can reduce the human and environmental risks associated with traditional approaches and deliver real-time data to water resource managers.

Data availability. All raw data can be provided by the corresponding authors upon request.

Supplement. The supplement related to this article is available online at: https://doi.org/10.5194/hess-27-1-2023-supplement.

Author contributions. NRH, RB, DW, JS, ND, AG, and SA conceptualised the work; NRH, RB, and DW curated and analysed the data; DW, JS, AG, and SA contributed to acquisition of the funding supporting this work; NRH, RB, DW, JS, ND, BE, AG, and SA contributed to the investigations of this work; NRH, RB, ND, BE, AG, and SA contributed to the methodology development; NRH, RB, DW, JS, BE, AG, and SA contributed to project administration; NRH, RB, DW, JS, BE, AG, and SA contributed to the provision of the project resources; NRH and BE contributed to the software development related to this work; JS, AG, and SA provided oversight and leadership in the supervision of the work; NRH, RB, and DW contributed to the validation of the research outputs; NRH prepared the visualisations and original draft of the published work; and RB, DW, JS, ND, BE, AG, and SA contributed review and editing of the work.

Competing interests. The contact author has declared that none of the authors has any competing interests.

Acknowledgements. The authors would like to thank James Mancey (Department of Natural Resources and Environment Tasmania, Australia) and Anthony Belcher (WaterNSW, Australia) for providing study sites and historical discharge gauging data. The authors would also like to thank Paul Blumer (Murrumbidgee Irrigation) for providing the example irrigation channel analysed in this study. This work was supported by Henry Valk's (IoTamy) and Nicolas Turner's (The University of Queensland, Australia) tireless efforts in the early development of the CVSG device integrated hardware solution, which collected a substantial portion of the data presented in this study. This research was supported by an Australian Government Research Training Program (RTP) Scholarship.

Review statement. This paper was edited by Roger Moussa and reviewed by Frank Engel and two anonymous referees.

References

Adelson, E. H., Burt, P. J., Anderson, C. H., Ogden, J. M., and Bergen, J. R.: Pyramid Methods in Image Processing, RCA Eng., 29, 33–41, 1984.

Albert, S., Kvennefors, C., Jacob, K., Kera, J., and Grinham, A.: Environmental change in a modified catchment downstream of a gold mine, Solomon Islands, Environ. Pollut., 231, 942–953, https://doi.org/10.1016/j.envpol.2017.08.113, 2017.

Albert, S., Deering, N., Tongi, S., Nandy, A., Kisi, A., Sirikolo, M., Maehaka, M., Hutley, N., Kies-Ryan, S., and Grinham, A.: Water quality challenges associated with industrial logging of a karst landscape: Guadalcanal, Solomon Islands, Mar. Pollut. Bull., 169, 112506, https://doi.org/10.1016/J.MARPOLBUL.2021.112506, 2021.

Baker, S., Scharstein, D., Lewis, J. P., Roth, S., Black, M. J., and Szeliski, R.: A database and evaluation methodology for optical flow, Int. J. Comput. Vision, 92, 1–31, https://doi.org/10.1007/S11263-010-0390-2, 2011.

Banasiak, R. and Krzyżanowski, M.: Flood flows in the Odra River in 2010 – quantitative and qualitative assessment of ADCP data, Meteorol. Hydrol. Water Manag. Res. Oper. Appl., 3, 11–20, 2015.

Bechle, A. J., Wu, C. H., Liu, W.-C., and Kimura, N.: Development and Application of an Automated River-Estuary Discharge Imaging System, J. Hydraul. Eng., 138, 327–339, https://doi.org/10.1061/(ASCE)HY.1943-7900.0000521, 2012.

Birgand, F., Lellouche, G., and Appelboom, T. W.: Measuring flow in non-ideal conditions for short-term projects: Uncertainties associated with the use of stage-discharge rating curves, J. Hydrol., 503, 186–195, https://doi.org/10.1016/j.jhydrol.2013.09.007, 2013.

Boiten, W.: Flow measurement structures, Flow Meas. Instrum., 13, 203–207, https://doi.org/10.1016/S0955-5986(02)00057-2, 2002.

Branch, M. A., Coleman, T. F., and Li, Y.: A Subspace, Interior, and Conjugate Gradient Method for Large-Scale Bound-Constrained Minimization Problems, SIAM J. Sci. Comput., 21, 1–23, https://doi.org/10.1137/S1064827595289108, 1999.

Cardona, J. L.: Visual Anemometry: Wind Speed Measurement Through Visual Observation of Fluid-Structure Interactions, Stanford University PP, United States, California, Ann Arbor, 144 pp., 2021.

Chen, C. Y., Wang, L., Hwang, C. H., Hsieh, C. W., and Chi, P. W.: Enhancing the performance of a rainfall measurement system using artificial neural networks based object tracking algorithms, in: I2MTC 2019 – 2019 IEEE International Instrumentation and Measurement Technology Conference, Proceedings, 1–4, https://doi.org/10.1109/I2MTC.2019.8827108, 2019.

Costa, J. E., Spicer, K. R., Cheng, R. T., Haeni, F. P., Melcher, N. B., Thurman, E. M., Plant, W. J., and Keller, W. C.: measuring stream discharge by non-contact methods: A Proof-of-Concept Experiment, Geophys. Res. Lett., 27, 553–556, https://doi.org/10.1029/1999GL006087, 2000.

Crochemore, L., Isberg, K., Pimentel, R., Pineda, L., Hasan, A., and Arheimer, B.: Lessons learnt from checking the quality of openly accessible river flow data worldwide, Hydrol. Sci. J., 65, 699–711, https://doi.org/10.1080/02626667.2019.1659509, 2020.

Daly, E., Calabrese, S., Yin, J., and Porporato, A.: Hydrological Spaces of Long-Term Catchment Wa-

ter Balance, Water Resour. Res., 55, 10747–10764, https://doi.org/10.1029/2019WR025952, 2019.

Despax, A., Le Coz, J., Hauet, A., Mueller, D. S., Engel, F. L., Blanquart, B., Renard, B., and Oberg, K. A.: Decomposition of Uncertainty Sources in Acoustic Doppler Current Profiler Streamflow Measurements Using Repeated Measures Experiments, Water Resour. Res., 55, 7520–7540, https://doi.org/10.1029/2019WR025296, 2019.

Detert, M.: How to Avoid and Correct Biased Riverine Surface Image Velocimetry, Water Resour. Res., 57, e2020WR027833, https://doi.org/10.1029/2020WR027833, 2021.

Di Baldassarre, G. and Montanari, A.: Uncertainty in river discharge observations: a quantitative analysis, Hydrol. Earth Syst. Sci., 13, 913–921, https://doi.org/10.5194/hess-13-913-2009, 2009.

Dobriyal, P., Badola, R., Tuboi, C., and Hussain, S. A.: A review of methods for monitoring streamflow for sustainable water resource management, Appl. Water Sci., 7, 2617–2628, https://doi.org/10.1007/s13201-016-0488-y, 2017.

Dramais, G., Le Coz, J., Camenen, B., and Hauet, A.: Advantages of a mobile LSPIV method for measuring flood discharges and improving stage-discharge curves, J. Hydro-Environ. Res., 5, 301–312, https://doi.org/10.1016/j.jher.2010.12.005, 2011.

Eltner, A., Elias, M., Sardemann, H., and Spieler, D.: Automatic Image-Based Water Stage Measurement for Long-Term Observations in Ungauged Catchments, Water Resour. Res., 54, 10362–10371, https://doi.org/10.1029/2018WR023913, 2018.

Eltner, A., Bressan, P. O., Akiyama, T., Gonçalves, W. N., and Marcato Junior, J.: Using Deep Learning for Automatic Water Stage Measurements, Water Resour. Res., 57, e2020WR027608, https://doi.org/10.1029/2020WR027608, 2021.

Farnebäck, G.: Polynomial expansion for orientation and motion estimation, Linköping University Electronic Press, Computer Vision, Department of Electrical Engineering, Linköping University, 181 pp., ISBN 91-7373-475-6, 2002.

Farnebäck, G.: Two-frame motion estimation based on polynomial expansion, Lect. Notes Comput. Sc., 2749, 363–370, https://doi.org/10.1007/3-540-45103-X_50, 2003.

Fenton, J. D.: On the generation of stream rating curves, J. Hydrol., 564, 748–757, https://doi.org/10.1016/J.JHYDROL.2018.07.025, 2018.

Fujita, I., Watanabe, H., and Tsubaki, R.: Development of a non-intrusive and efficient flow monitoring technique: The space-time image velocimetry (STIV), Int. J. River Basin Manag., 5, 105–114, https://doi.org/10.1080/15715124.2007.9635310, 2007.

Fujita, I. and Komura, S.: Application of Video Image Analysis for Measurements of River-Surface Flows, Proc. Hydraul. Eng., 38, 733–738, https://doi.org/10.2208/prohe.38.733, 1994.

Gaume, E., Bain, V., Bernardara, P., Newinger, O., Barbuc, M., Bateman, A., Blaškovičová, L., Blöschl, G., Borga, M., Dumitrescu, A., Daliakopoulos, I., Garcia, J., Irimescu, A., Kohnova, S., Koutroulis, A., Marchi, L., Matreata, S., Medina, V., Preciso, E., Sempere-Torres, D., Stancalie, G., Szolgay, J., Tsanis, I., Velasco, D., and Viglione, A.: A compilation of data on European flash floods, J. Hydrol., 367, 70–78, https://doi.org/10.1016/J.JHYDROL.2008.12.028, 2009.

Gordon, R. L.: Acoustic Measurement of River Discharge, J. Hydraul. Eng., 115, 925–936, https://doi.org/10.1061/(asce)0733-9429(1989)115:7(925), 1989.

Grinham, A. R.: Downstream effects of land use on shallow-water benthic microalgal communities in Moreton Bay, Australia and Marovo Lagoon, PhD thesis, Solomon Islands, https://espace.library.uq.edu.au/view/UQ:158525 TS5, 2007.

Grinham, A., Gibbes, B., Gale, D., Watkinson, A., and Bartkow, M.: Extreme rainfall and drinking water quality: A regional perspective, WIT Trans. Ecol. Envir., 164, 183–194, https://doi.org/10.2495/WP120161, 2012.

Guerrero, J.-L., Westerberg, I. K., Halldin, S., Xu, C.-Y., and Lundin, L.-C.: Temporal variability in stage–discharge relationships, J. Hydrol., 446–447, 90–102, https://doi.org/10.1016/j.jhydrol.2012.04.031, 2012.

Harding, S. F., Richmond, M. C., Romero-Gomez, P., and Serkowski, J. A.: Effects of non-homogeneous flow on ADCP data processing in a hydroturbine forebay, Flow Meas. Instrum., 52, 1–9, https://doi.org/10.1016/J.FLOWMEASINST.2015.12.010, 2016.

Hauet, A., Creutin, J.-D., and Belleudy, P.: Sensitivity study of large-scale particle image velocimetry measurement of river discharge using numerical simulation, J. Hydrol., 349, 178–190, https://doi.org/10.1016/j.jhydrol.2007.10.062, 2008.

Hauet, A., Morlot, T., and Daubagnan, L.: Velocity profile and depth-averaged to surface velocity in natural streams: A review over a large sample of rivers, E3S Web Conf., 40, 06015, https://doi.org/10.1051/e3sconf/20184006015, 2018.

Hering, D., Carvalho, L., Argillier, C., Beklioglu, M., Borja, A., Cardoso, A. C., Duel, H., Ferreira, T., Globevnik, L., Hanganu, J., Hellsten, S., Jeppesen, E., Kodeš, V., Solheim, A. L., Nõges, T., Ormerod, S., Panagopoulos, Y., Schmutz, S., Venohr, M., and Birk, S.: Managing aquatic ecosystems and water resources under multiple stress – An introduction to the MARS project, Sci. Total Environ., 503–504, 10–21, 2015.

Herrera, D., Ellis, A., Fisher, B., Golden, C. D., Johnson, K., Mulligan, M., Pfaff, A., Treuer, T., and Ricketts, T. H.: Upstream watershed condition predicts rural children's health across 35 developing countries, Nat. Commun., 8, 811, https://doi.org/10.1038/s41467-017-00775-2, 2017.

Herschy, R.: The velocity-area method, Flow Meas. Instrum., 4, 7–10, https://doi.org/10.1016/0955-5986(93)90004-3, 1993.

Hutley, N., Boselalu, M., Wenger, A., Grinham, A., Gibbes, B., and Albert, S.: Evaluating the effect of data-richness and model complexity in the prediction of coastal sediment loading in Solomon Islands, Environ. Res. Lett., 15, 124044, https://doi.org/10.1088/1748-9326/ABC8BA, 2020.

Jackson, E. K., Roberts, W., Nelsen, B., Williams, G. P., Nelson, E. J., and Ames, D. P.: Introductory overview: Error metrics for hydrologic modelling – A review of common practices and an open source library to facilitate use and adoption, Environ. Modell. Softw., 119, 32–48, https://doi.org/10.1016/J.ENVSOFT.2019.05.001, 2019.

Jalbert, J., Mathevet, T., and Favre, A.-C.: Temporal uncertainty estimation of discharges from rating curves using a variographic analysis, J. Hydrol., 397, 83–92, https://doi.org/10.1016/j.jhydrol.2010.11.031, 2011.

Jiang, S., Babovic, V., Zheng, Y., and Xiong, J.: Advancing Opportunistic Sensing in Hydrology: A Novel Approach to Measuring Rainfall With Ordinary Surveillance Cameras, Water Resour.

Res., 55, 3004–3027, https://doi.org/10.1029/2018WR024480, 2019.

Khalid, M., Pénard, L., and Mémin, E.: Optical flow for image-based river velocity estimation, Flow Meas. Instrum., 65, 110–121, https://doi.org/10.1016/j.flowmeasinst.2018.11.009, 2019.

Kiang, J. E., Gazoorian, C., McMillan, H., Coxon, G., Le Coz, J., Westerberg, I. K., Belleville, A., Sevrez, D., Sikorska, A. E., Petersen-Øverleir, A., Reitan, T., Freer, J., Renard, B., Mansanarez, V., and Mason, R.: A Comparison of Methods for Streamflow Uncertainty Estimation, Water Resour. Res., 54, 7149–7176, https://doi.org/10.1029/2018WR022708, 2018.

Klema, M. R., Pirzado, A. G., Venayagamoorthy, S. K., and Gates, T. K.: Analysis of acoustic Doppler current profiler mean velocity measurements in shallow flows, Flow Meas. Instrum., 74, 101755, https://doi.org/10.1016/j.flowmeasinst.2020.101755, 2020.

Koutalakis, P., Tzoraki, O., and Zaimes, G.: Uavs for hydrologic scopes: Application of a low-cost UAV to estimate surface water velocity by using three different image-based methods, Drones, 3, 1–15, https://doi.org/10.3390/DRONES3010014, 2019.

Kuentz, A., Arheimer, B., Hundecha, Y., and Wagener, T.: Understanding hydrologic variability across Europe through catchment classification, Hydrol. Earth Syst. Sci., 21, 2863–2879, https://doi.org/10.5194/hess-21-2863-2017, 2017.

Le Coz, J., Hauet, A., Pierrefeu, G., Dramais, G., and Camenen, B.: Performance of image-based velocimetry (LSPIV) applied to flash-flood discharge measurements in Mediterranean rivers, J. Hydrol., 394, 42–52, 2010.

Le Coz, J., Renard, B., Vansuyt, V., Jodeau, M., and Hauet, A.: Estimating the uncertainty of video-based flow velocity and discharge measurements due to the conversion of field to image coordinates, Hydrol. Process., 35, e14169, https://doi.org/10.1002/hyp.14169, 2021.

Lee, K., Ho, H.-C., Marian, M., and Wu, C.-H.: Uncertainty in open channel discharge measurements acquired with StreamPro ADCP, J. Hydrol., 509, 101–114, https://doi.org/10.1016/j.jhydrol.2013.11.031, 2014.

Lee, M.-C., Leu, J.-M., Chan, H.-C., and Huang, W.-C.: The measurement of discharge using a commercial digital video camera in irrigation canals, Flow Meas. Instrum., 21, 150–154, https://doi.org/10.1016/j.flowmeasinst.2010.02.002, 2010.

Leeuw, T. and Boss, E.: The HydroColor App: Above Water Measurements of Remote Sensing Reflectance and Turbidity Using a Smartphone Camera, Sensors, 18, 256, https://doi.org/10.3390/s18010256, 2018.

Lehmann, J., Coumou, D., and Frieler, K.: Increased record-breaking precipitation events under global warming, Clim. Change, 132, 501–515, https://doi.org/10.1007/S10584-015-1434-Y, 2015.

Leitão, J. P., Peña-Haro, S., Lüthi, B., Scheidegger, A., and Moy de Vitry, M.: Urban overland runoff velocity measurement with consumer-grade surveillance cameras and surface structure image velocimetry, J. Hydrol., 565, 791–804, https://doi.org/10.1016/j.jhydrol.2018.09.001, 2018.

Li, S., Sparrow, S. N., L, F. E., Gudmundsson, L., and Seneviratne, S. I.: Anthropogenic climate change affects meteorological drought risk in Europe, Environ. Res. Lett., 11, 044005, https://doi.org/10.1088/1748-9326/11/4/044005, 2016.

Li, W., Liao, Q., and Ran, Q.: Stereo-imaging LSPIV (SI-LSPIV) for 3D water surface reconstruction and discharge measurement in mountain river flows, J. Hydrol., 578, 124099, https://doi.org/10.1016/j.jhydrol.2019.124099, 2019.

Lindow, N. L. and Curtis, M. C.: Developing a framework for watershed implementation plans, in: ASABE – TMDL 2010: Watershed Management to Improve Water Quality Proceedings, Hyatt Regency Baltimore on the Inner Harbor, Baltimore, Maryland, USA, 14–17 November 2010, 133–141, https://doi.org/10.13031/2013.35749, 2010.

Mcmillan, H., Krueger, T., and Freer, J.: Benchmarking observational uncertainties for hydrology: Rainfall, river discharge and water quality, Hydrol. Process., 26, 4078–4111, 2012.

Mueller, M., Pander, J., and Geist, J.: The effects of weirs on structural stream habitat and biological communities, J. Appl. Ecol., 48, 1450–1461, https://doi.org/10.1111/J.1365-2664.2011.02035.X, 2011.

Naves, J., García, J. T., Puertas, J., and Anta, J.: Assessing different imaging velocimetry techniques to measure shallow runoff velocities during rain events using an urban drainage physical model, Hydrol. Earth Syst. Sci., 25, 885–900, https://doi.org/10.5194/hess-25-885-2021, 2021.

Nearing, G. S. and Gupta, H. V.: Ensembles vs. information theory: supporting science under uncertainty, Front Earth Sci.-Prc., 12, 653–660, https://doi.org/10.1007/s11707-018-0709-9, 2018.

Nemade, N. and Gohokar, V. V.: Comparative Performance Analysis of Optical Flow Algorithms for Anomaly Detection, in: Proceedings of International Conference on Communication and Information Processing (ICCIP), 18 May 2019, https://doi.org/10.2139/ssrn.3419775, 2019.

Oberg, K. and Mueller, D. S.: Validation of Streamflow Measurements Made with Acoustic Doppler Current Profilers, J. Hydraul. Eng., 133, 1421–1432, https://doi.org/10.1061/(ASCE)0733-9429(2007)133:12(1421), 2007.

Ogden, F. L., Crouch, T. D., Pradhan, N. R., and Kempema, E.: Laboratory Investigation of Sedimentation Effects on V-Notch Weirs, Bear. Knowl. Sustain. – Proc. 2011 World Environ. Water Resour. Congr., Palm Springs, California, 22–26 May 2011, 4820–4827, https://doi.org/10.1061/41173(414)500, 2011.

Pagliara, S. and Palermo, M.: Scour problems downstream of low-head hydraulic structures, in: Rivers – Physical, Fluvial and Environmental Processes, 99–119, https://doi.org/10.1007/978-3-319-17719-9_4, 2015.

Palmer, T. N. and Räisänen, J.: Quantifying the risk of extreme seasonal precipitation events in a changing climate, Nature, 415, 512–514, https://doi.org/10.1038/415512a, 2002.

Park, S. Y., Sur, C., Kim, J. S., Choi, S. J., Lee, J. H., and Kim, T. W.: Projected drought risk assessment from water balance perspectives in a changing climate, Int. J. Climatol., 41, 2765–2777, https://doi.org/10.1002/JOC.6988, 2021.

Peacock, M., Audet, J., Bastviken, D., Futter, M. N., Gauci, V., Grinham, A., Harrison, J. A., Kent, M. S., Kosten, S., Lovelock, C. E., Veraart, A. J., and Evans, C. D.: Global importance of methane emissions from drainage ditches and canals, Environ. Res. Lett., 16, 044010, https://doi.org/10.1088/1748-9326/ABEB36, 2021.

Pearce, S., Ljubičić, R., Peña-Haro, S., Perks, M., Tauro, F., Pizarro, A., Dal Sasso, S., Strelnikova, D., Grimaldi, S., Maddock, I., Paulus, G., Plavšić, J., Prodanović, D., and Man-

freda, S.: An Evaluation of Image Velocimetry Techniques under Low Flow Conditions and High Seeding Densities Using Unmanned Aerial Systems, Remote Sens.-Basel, 12, 232, https://doi.org/10.3390/rs12020232, 2020.

Peña-Haro, S., Carrel, M., Lüthi, B., Hansen, I., and Lukes, R.: Robust Image-Based Streamflow Measurements for Real-Time Continuous Monitoring, Front. Water, 3, 766918, https://doi.org/10.3389/FRWA.2021.766918, 2021.

Perks, M. T.: KLT-IV v1.0: image velocimetry software for use with fixed and mobile platforms, Geosci. Model Dev., 13, 6111–6130, https://doi.org/10.5194/gmd-13-6111-2020, 2020a.

Perks, M. T., Dal Sasso, S. F., Hauet, A., Jamieson, E., Le Coz, J., Pearce, S., Peña-Haro, S., Pizarro, A., Strelnikova, D., Tauro, F., Bomhof, J., Grimaldi, S., Goulet, A., Hortobágyi, B., Jodeau, M., Käfer, S., Ljubičić, R., Maddock, I., Mayr, P., Paulus, G., Pénard, L., Sinclair, L., and Manfreda, S.: Towards harmonisation of image velocimetry techniques for river surface velocity observations, Earth Syst. Sci. Data, 12, 1545–1559, https://doi.org/10.5194/essd-12-1545-2020, 2020b.

Petrie, J., Diplas, P., Gutierrez, M., and Nam, S.: Data evaluation for acoustic Doppler current profiler measurements obtained at fixed locations in a natural river, Water Resour. Res., 49, 1003–1016, https://doi.org/10.1002/wrcr.20112, 2013.

Pizarro, A., Dal Sasso, S. F., Perks, M. T., and Manfreda, S.: Identifying the optimal spatial distribution of tracers for optical sensing of stream surface flow, Hydrol. Earth Syst. Sci., 24, 5173–5185, https://doi.org/10.5194/hess-24-5173-2020, 2020.

Prüss-Ustün, A., Bartram, J., Clasen, T., Colford, J. M., Cumming, O., Curtis, V., Bonjour, S., Dangour, A. D., De France, J., Fewtrell, L., Freeman, M. C., Gordon, B., Hunter, P. R., Johnston, R. B., Mathers, C., Mäusezahl, D., Medlicott, K., Neira, M., Stocks, M., Wolf, J., and Cairncross, S.: Burden of disease from inadequate water, sanitation and hygiene in low- and middle-income settings: A retrospective analysis of data from 145 countries, Trop. Med. Int. Health, 19, 894–905, https://doi.org/10.1111/tmi.12329, 2014.

Pumo, D., Alongi, F., Ciraolo, G., and Noto, L.: Optical Methods for River Monitoring: A Simulation-Based Approach to Explore Optimal Experimental Setup for LSPIV, Water, 13, 247, https://doi.org/10.3390/w13030247, 2021.

Rahman Khan, M., Gourley, J. J., Duarte, J. A., Vergara, H., Wasielewski, D., Ayral, P.-A., and Fulton, J. W.: Uncertainty in remote sensing of streams using noncontact radars, J. Hydrol., 603, 126809, https://doi.org/10.1016/j.jhydrol.2021.126809, 2021.

Ran, Q. H., Li, W., Liao, Q., Tang, H. L., and Wang, M. Y.: Application of an automated LSPIV system in a mountainous stream for continuous flood flow measurements, Hydrol. Process., 30, 3014–3029, https://doi.org/10.1002/HYP.10836, 2016.

Savitzky, A. and Golay, M. J. E.: Smoothing and Differentiation of Data by Simplified Least Squares Procedures, Anal. Chem., 36, 1627–1639, https://doi.org/10.1021/AC60214A047, 1964.

Schmid, M., Rath, D., and Diebold, U.: Why and How Savitzky–Golay Filters Should Be Replaced, ACS Meas. Sci. Au, 2, 185–196, https://doi.org/10.1021/ACSMEASURESCIAU.1C00054, 2022.

Sene, K., Tych, W., and Beven, K.: Exploratory studies into seasonal flow forecasting potential for large lakes, Hydrol. Earth Syst. Sci., 22, 127–141, https://doi.org/10.5194/hess-22-127-2018, 2018.

Shah, S. T. H. and Xuezhi, X.: Traditional and modern strategies for optical flow: an investigation, SN Appl. Sci., 3, 289, https://doi.org/10.1007/s42452-021-04227-x, 2021.

Shi, R., Leng, X., and Chanson, H.: On optical flow techniques applied to breaking surges, Flow Meas. Instrum., 72, 101710, https://doi.org/10.1016/j.flowmeasinst.2020.101710, 2020.

Steinbakk, G. H., Thorarinsdottir, T. L., Reitan, T., Schlichting, L., Hølleland, S., and Engeland, K.: Propagation of rating curve uncertainty in design flood estimation, Water Resour. Res., 52, 6897–6915, https://doi.org/10.1002/2015WR018516, 2016.

Stumpf, A., Augereau, E., Delacourt, C., and Bonnier, J.: Photogrammetric discharge monitoring of small tropical mountain rivers: A case study at Rivière des Pluies, Réunion Island, Water Resour. Res., 52, 4550–4570, https://doi.org/10.1002/2015WR018292, 2016.

Tauro, F., Petroselli, A., Porfiri, M., Giandomenico, L., Bernardi, G., Mele, F., Spina, D., and Grimaldi, S.: A novel permanent gauge-cam station for surface-flow observations on the Tiber River, Geosci. Instrum. Method. Data Syst., 5, 241–251, https://doi.org/10.5194/gi-5-241-2016, 2016.

Tauro, F., Petroselli, A., and Grimaldi, S.: Optical sensing for stream flow observations: A review, J. Agr. Eng., 49, 199–206, https://doi.org/10.4081/jae.2018.836, 2018.

Tomkins, K. M.: Uncertainty in streamflow rating curves: methods, controls and consequences, Hydrol. Process., 28, 464–481, https://doi.org/10.1002/hyp.9567, 2014.

Wang, S. and Miao, Z.: Anomaly detection in crowd scene, Int. Conf. Signal Process. Proceedings, ICSP, Beijing, China, 24–28 October 2010, 1220–1223, https://doi.org/10.1109/ICOSP.2010.5655356, 2010.

Wang, X., Wang, M., Liu, X., Zhu, L., Glade, T., Chen, M., Zhao, W., and Xie, Y.: A novel quality control model of rainfall estimation with videos – A survey based on multi-surveillance cameras, J. Hydrol., 605, 127312, https://doi.org/10.1016/j.jhydrol.2021.127312, 2022.

Watanabe, K., Fujita, I., Iguchi, M., and Hasegawa, M.: Improving Accuracy and Robustness of Space-Time Image Velocimetry (STIV) with Deep Learning, Water, 13, 2079, https://doi.org/10.3390/W13152079, 2021.

Westerberg, I., Guerrero, J.-L., Seibert, J., Beven, K. J., and Halldin, S.: Stage-discharge uncertainty derived with a non-stationary rating curve in the Choluteca River, Honduras, Hydrol. Process., 25, 603–613, https://doi.org/10.1002/hyp.7848, 2011.

Westerberg, I. K., Wagener, T., Coxon, G., McMillan, H. K., Castellarin, A., Montanari, A., and Freer, J.: Uncertainty in hydrological signatures for gauged and ungauged catchments, Water Resour. Res., 52, 1847–1865, https://doi.org/10.1002/2015WR017635, 2016.

Yang, Y., Wen, B., Wang, C., and Hou, Y.: Real-Time and Automatic River Discharge Measurement with UHF Radar, IEEE Geosci. Remote S, 17, 1851–1855, https://doi.org/10.1109/LGRS.2019.2958082, 2020.

Remarks from the language copy-editor

CE1   Please note that this unhyphenated version of the noun is our house standard.

CE2   This is the correct form since here the word functions as a noun.

Remarks from the typesetter

TS1   I have inserted your changes to the following section. Please check again if all vectors are correctly denoted by bold italics and matrices by bold roman.

TS2   Please give an explanation of why this needs to be changed. We have to ask the handling editor for approval. Thanks.

TS3   Please give an explanation of why this needs to be changed. We have to ask the handling editor for approval. Thanks.

TS4   The units in this figure do not need to be changed to exponential format in figures as we only change those instances throughout the text.

TS5   Please provide last access date.